2012

Ultrasonic Concentration of Microorganisms

Samuel J. Mullins
University of Kentcuky, samueljmullins@gmail.com

STUDENT AGREEMENT:

I represent that my thesis or dissertation and abstract are my original work. Proper attribution has been given to all outside sources. I understand that I am solely responsible for obtaining any needed copyright permissions. I have obtained and attached hereto needed written permission statements(s) from the owner(s) of each third-party copyrighted matter to be included in my work, allowing electronic distribution (if such use is not permitted by the fair use doctrine).

I hereby grant to The University of Kentucky and its agents the non-exclusive license to archive and make accessible my work in whole or in part in all forms of media, now or hereafter known. I agree that the document mentioned above may be made available immediately for worldwide access unless a preapproved embargo applies.

I retain all other ownership rights to the copyright of my work. I also retain the right to use in future works (such as articles or books) all or part of my work. I understand that I am free to register the copyright to my work.

REVIEW, APPROVAL AND ACCEPTANCE

The document mentioned above has been reviewed and accepted by the student's advisor, on behalf of the advisory committee, and by the Director of Graduate Studies (DGS), on behalf of the program; we verify that this is the final, approved version of the student's dissertation including all changes required by the advisory committee. The undersigned agree to abide by the statements above.

Samuel J. Mullins, Student

Dr. Fred A. Payne, Major Professor

Dr. Dwayne Edwards, Director of Graduate Studies

Ultrasonic Concentration of Microorganisms

THESIS

A thesis submitted in partial fulfillment of the requirements for the degree of
Master of Science in Biosystems and Agricultural Engineering
in the College of Engineering at the University of Kentucky.

By

Samuel James Mullins

Lexington, Kentucky

Director: Dr. Fred A. Payne,

Professor of Biosystems and Agricultural Engineering

Lexington, Kentucky

2012

ABSTRACT OF THESIS

ULTRASONIC CONENTRATION OF MICROOGANISMS

Concentration of microorganisms from a sample volume would increase the limits of detection of samples used for rapid-detection methods. Rapid detection methods are is advantageous for the food industry to rapidly test for bacteria in order release products on a timely basis. Ultrasonic concentration was considered a promising method for manipulation of microorganisms. An ultrasonic chamber consisting of parallel piezoceramic discs with a reticulated polyurethane foam mesh was used to concentrate *Saccharomyces cerevisiae* yeast and *Escherichia coli* bacteria. The concentration of yeast was seen to increase by 200% (from 8.0×10^4 cells mL^{-1} to 2.4×10^5 cells mL^{-1}) while almost zero concentration of bacteria was observed. The poor concentration effect seen with the smaller microorganisms was explained by the volume dependent acoustic radiation force exerted on the particles; the concentration forces are 1,000 times smaller for a 1 μm bacteria cell versus a 10 μm yeast cell.

KEYWARDS: Ultrasonic Concentration, Ultrasonic Standing Wave, Bacterial Concentration, Yeast Concentration, Reticulated Polyurethane Foam Mesh.

Samuel James Mullins

9-26-2012

ULTRASONIC CONCENTRATION OF MICROORGANISMS

By

Samuel James Mullins

Dr. Fred A. Payne
(Director of Thesis)

Dr. Dwayne Edwards
(Director of Graduate Studies)

Samuel James Mullins

TABLE OF CONTENTS

LIST OF TABLES

LIST OF FIGURES

CHAPTER 1 : INTRODUCTION

1.1 Research Goal

The goal of this research was to explore the use of ultrasonic concentration with bacterial food pathogens in order to enhance the detection limits of rapid detection methods.

1.2 Rapid Detection of Food Pathogens

Contamination of food products from bacterial pathogens will always be a problem. Often, food testing is challenged with finding very small amounts of bacteria in very large quantities of food. Complicating matters further, it is advantageous for the food industry to rapidly test for bacteria in order release products on a timely basis.

The traditional method of pathogen detection from a sample can take two to six days. Newer techniques using polymerase chain reaction (PCR) and nucleic acid sequence-based amplification (NASBA) can be completed in two to six hours. However, the PCR and NASBA have a minimum detection limit of 10^3-10^4 colony forming units per milliliter (CFU mL^{-1}), while the FDA has implemented a zero-tolerance policy for food-borne pathogens. Cultural enrichment would be a necessary and time consuming step in order to determine if there are any microbial pathogens present in the sample. Typical volumes used for the rapid-detection methods range between 0.1-1.0 mL taken from a much larger representative sample (usually greater than 25 mL) from the original food sample which is usually 20 g. This means a 25- to 250-fold decrease in volume with a 100% recovery of bacterial pathogens from the original food sample would be ideal (Jaykus, 2003).

1.3 Acoustic Waves

Humans know sound as the perception of small pressure difference transmitted through air as longitudinal waves also known as compression waves or acoustic waves. These pressure waves hit the eardrum, imparting movement to the basilar membrane. The basilar membrane, located in the cochlea of the inner ear, furthermore sends signals to the cochlear nerve, or auditory nerve, which in turn sends information to the brain. Humans can perceive sound frequencies between 20 hertz and 20,000 hertz (20Hz-

20kHz). Sound beyond human audible perception is classified as "ultrasound" or greater than 20 kHz while "infrasound" is less than 20Hz (0-20Hz).

Acoustic waves have three fundamental properties from which other properties can be calculated: frequency, wavelength and speed of propagation. The speed at which a wave propagates are different between materials and relates to the material's density and compressibility. The speed of an acoustic wave (c) is defined in Equation 1.1 as a relation of the change in pressure (ΔP) multiplied by the initial volume (V) to the change in volume (ΔV) multiplied by the density (ρ).

$$c = \sqrt{\frac{(\Delta P)(V)}{(\Delta V)(\rho)}} \qquad 1.1$$

The speed of sound varies by material type and temperature. In general, the speed of sound increased as the density of the material increases. Higher temperatures generally decrease the speed of sound based on the thermal expansion and density decrease of that material. The speed of sound for common materials at room temperature are shown in Table 1.1.

Table 1.1 Common materials and their speed of sound (Serway and Jewett 2004:513)

Material	Speed of Sound, c ($m\ s^{-1}$)
Air	343
Fresh Water	1,493
Sea Water	1,533
Iron	5,950

A propagating acoustic wave is defined as a wave that carries energy from one point to another; a speaker sending waves to someone's eardrums, for example. An acoustic wave will propagate in a medium until it is loses all its energy to attenuation and friction between molecules or when the wave encounters another object, or discontinuity. When a propagating wave hits an object, some of the wave is transmitted into the object and some is reflected back. A simple example of an object would be a wall which reflects a wave with little or no acoustic impedance or losses from reflection.

Standing waves are created when the reflected waves interact constructively with the forward wave; this happens only when the frequency and wavelength are correct for a

given distance. See Figure 1.1 for an example of four different standing wave frequencies over a given length, *l*.

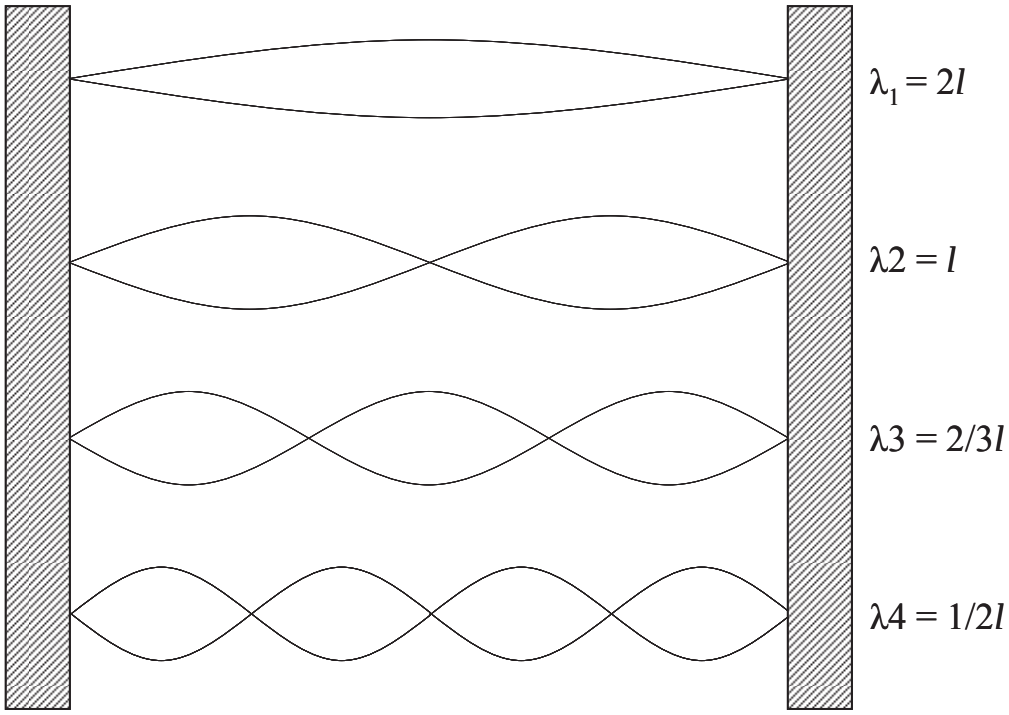

Figure 1.1 Representation of the standing wave of a string.

1.4 Piezoelectrics and Piezoceramics

Piezoelectricity was first demonstrated in 1880 by Peter Curie and Jacques Curie, when they demonstrated the electric polarization of specific crystalline minerals subjected to mechanical force. A material with a natural piezoelectric effect is silicon dioxide (SO_2), commonly known as quartz crystal. The applied mechanical force to the crystalline minerals is proportional to the electrical voltage potential created; the voltage generated compression and tension is opposite. Conversely, application of an electric voltage across the crystalline creates deformation. The lengthening and shortening of the crystalline is proportional to the polarity and strength of the electric potential – this is known as the inverse piezoelectric effect. Piezo- was derived from the Greek word *piezein*, which meant to press or to squeeze.

Comparing other actuators such as electric solenoids or hydraulic actuators, forces and movements produced by piezoelectric crystals are very small in magnitude; a piezoceramic disc will generally only displace a fraction of a micrometer per millimeter

of thickness. Values for a ceramics *piezoelectric constant* are given in picometers per volt; typical values range between 200 and 600 x 10^{-12} mV^{-1} (APC International Ltd. 2002:30). Relative to the thickness of a piezoceramic the displacements are fractions of nanometers per volt per millimeter of ceramic (0.2 to 0.6 $nmV^{-1}mm^{-1}$). Given an example of a ten millimeter (10 mm) thick ceramic disc and an application of 1000 volts, two-to-six micrometers (2-6 μm) of deflection will be imparted.

In 1915, the first useful piezoelectric device was sonar; the device used a layer of quartz crystal to send ultrasonic pulses into water, wait for a return, and then use the time difference between reflection and echo to calculate the distance to an underwater object. After this useful invention, there was great scientific interest in piezoelectrics, piezoelectric materials, and the hunt for new piezoelectric materials. An interesting invention was the "ultrasonic time-domain reflectometers" which were used to find discontinuities or flaws in a metal casting after sending an ultrasonic pulse through the material and any signal received before bouncing off the "far end" of the shape would be considered a discontinuity.

During and after World War II, there was great demand for man-made piezoelectric materials to be used for wartime development of new technologies (particularly in radio communication for durable and lightweight speakers and microphones). Researchers in the United States, Russia, and Japan developed barium titanate ($BaTiO_3$) and lead zirconate titanate or "PZT" ($Pb[Zr_{(x)}Ti_{(1-x)}]O_3$). The structure of a PZT piezoceramic cubic crystalline lattice is shown in Figure 1.2. A tetravalent zirconium or titanium ion is in the middle of an octahedron of oxygen, surrounded by divalent lead ions. The left side of Figure 1.2 shows the symmetric arrangement of positive and negative charges while the right side shows the stretched lattice having an electric dipole (APC International, 2002:6).

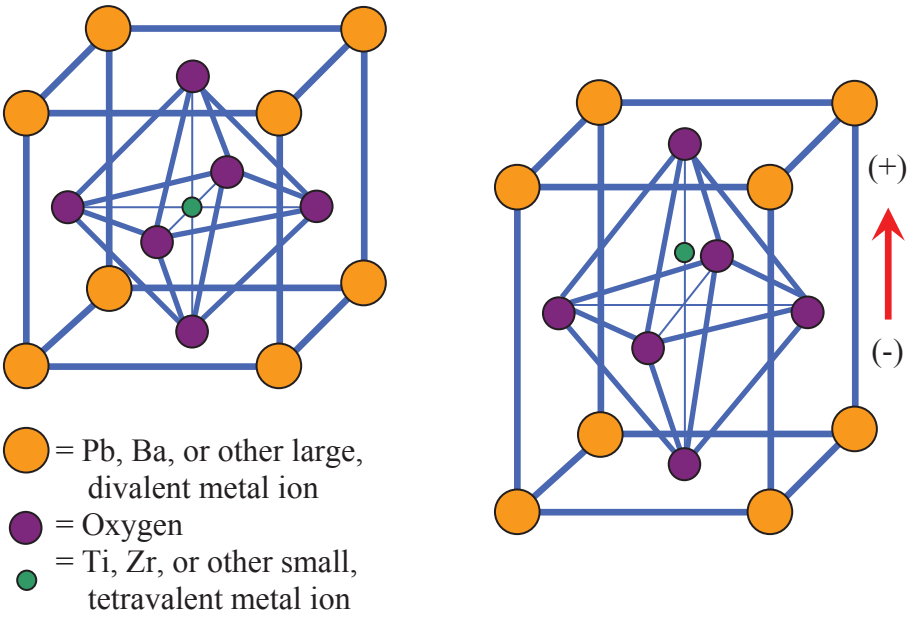

Figure 1.2 Cubic lattice structure of a piezoceramic crystal

Compared to quartz crystal, the piezoceramics are hundreds of times more sensitive to a force/voltage application see Table 1.2. The Relative Dielectric Constant (K) is the permittivity of the ceramic material divided by the permittivity of free space (8.85×10^{-12} farad per meter). The Electromechanical Coupling Factor (k_{33}) is the amount of mechanical energy converted per amount of electrical energy input, or conversely electrical energy converted per unit of mechanical force input. The Piezoelectric Charge Constant (d_{33}) is the electric field generated by the unit area of ceramic per amount of stress applied, or conversely the strain in the ceramic due to an applied electrical field.

Table 1.2 Properties of various Piezoelectrics (APC International Ltd. 2002:30)

Material	Relative Dielectric Constant (K) (unitless)	Electromechanical Coupling Factor (k33) (%)	Piezoelectric Charge Constant (d33) (10-12m/V)
Quartz	5	0.09	2.3
APC 840 Ceramic	1250	0.72	290
APC 856 Ceramic.	4100	0.73	620

1.5 History and Theory of Ultrasonic Particle Manipulation

Kundt and Lehman (1874) described acoustic radiation force in their experiment in which they trapped dust particles in a tube by applying a standing-wave field. Particles were collected in lateral lines along the length of the tube and were separated by a distance of half the wavelength of the sound wave.

King (1934) presented the first calculation of acoustic radiation forces on a small rigid sphere in an inviscous fluid within a standing wave. His theory predicted that particles would move toward the node or antinode of the field depending on the relative density factor, a function of the ratio of the densities of the particle and fluid. For a ratio of less than 0.4 (particle:fluid-density) then the acoustic force acts towards the pressure antinode. For a ratio greater than 0.4, the acoustic radiation force acts towards the pressure node. In his theory, King added gravity, Stokes drag forces, and radiation pressure to predict the path of small particles falling through acoustic fields and his predictions were shown to agree with experimental results for solid spheres suspended in gases but presented large errors with non-rigid spheres (Leung et al., 1981).

Yosioka and Kawashima extended King's theory to apply to compressible spheres. Westervelt (1951) applied the theory to the case of objects with arbitrary shapes, and Embleton (1953) applied it to cylindrical and spherical progressive wave fields. Nyborg (1967) was one of the first to apply the theory to the acoustic trapping of biological particles by presenting a derivation of the radiation force acting on a small rigid sphere.

1.6 Limitations of Ultrasonic Particle Manipulation

1.6.1 Particles

Resonant chambers for particle manipulation are designed to provide certain acoustic characteristics when they are filled with the fluid of interest, however, the acoustic characteristics are different for the fluid and the fluid/particle mix. Concentration differences will alter the acoustic field and individual particles may influence resonance frequency (Leung et al 1981). The required resonance may require the implementation of

automatic frequency control in order to maintain the concentrated particles at the pressure nodes. Further complications arise when the particles differ acoustically from the fluid, in which agglomerations can cause a breakdown of the acoustic field, thus losing the concentration of particles at the pressure nodes (Groschl 1998b).

1.6.2 Temperature

Temperature changes are also a factor to consider in ultrasonic particle manipulation. Temperature increases occur due to energy dissipation in the transducer and acoustic energy absorption. Temperature rises vary depending on input power, resonator size, and transducer material. Bubbles tend to form at elevated temperatures in microfluidic devices. Convection resulting from temperature increases can alter the order of particles. In some cases, mechanical failure of devices can occur. Doblhoffdier *et al.* (1994) had to implement an integrated cooling circuit in order to prevent temperature rises in the large chamber designed to retain mammalian cells. Bazou et al. (2005) on the other hand, reported less than 0.5 K temperature increase in their microscale chambers.

1.6.3 Viscosity

Fluid viscosity effects result from losses within the boundary layer of the sphere and are particularly significant for nanometer size spheres and low frequencies (~kHz). Doinikov (1997) derived a general expression for acoustic radiation forces in viscous and thermally conducting fluids looking specifically at plane progressive, plane standing, and spherically diverging fields. He was able to show that viscosity and thermal effects were minor for small and rigid spheres. Doinikov showed that in most applications of solid particle manipulation in water-based media, the effect of viscosity is negligible.

1.7 Applications of Ultrasonic Concentration

Ultrasonic concentration systems concentrate micro particles using acoustic forces to create and maintain a standing node; this standing pressure wave is created by a sound source (typically a piezoceramic element) to push particles to nodal planes in the chamber. Figure 1.3 illustrates a typical standing node. The source sound (P) is mounted parallel to the reflector. There are nodes of high pressure and antinodes of low pressure created. The microorganisms that have a specific gravity greater than the media are forced to the high pressure nodes.

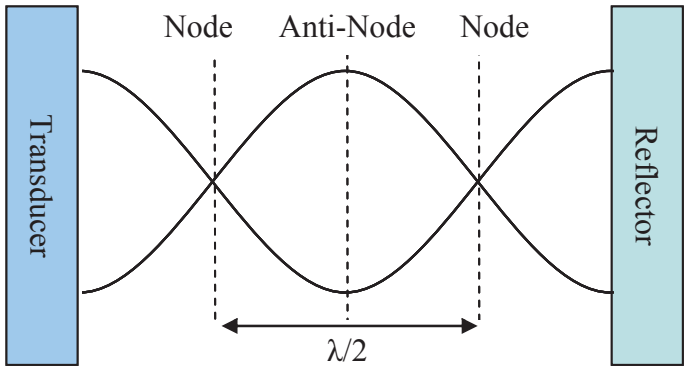

Figure 1.3 Schematic of a chamber with a standing acoustic wave

All of the applications of ultrasonic concentration rely upon the acoustic radiation forces acting on particles and moving thing to nodes or antinodes in the acoustic chamber. A representation of this can be seen in Figure 1.4.

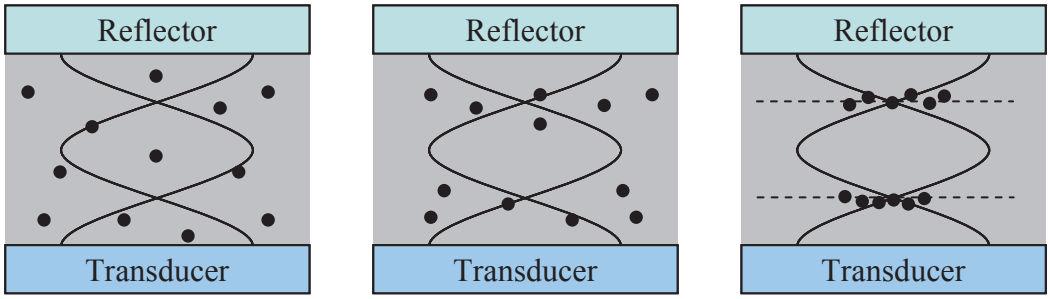

Figure 1.4 Example of particles with a density greater than the fluid forced towards nodes in an ultrasonic standing wave

1.7.1 Sedimentation

Particle filtration and concentration are common uses for ultrasonic radiation forces. In some cases it is desired to remove particles from a fluid medium or to concentrate them for further analysis. Until the late 1990's, the most common ultrasonic filtration technique was allowing particles to agglomerate under axial, lateral, and secondary ultrasonic forces. The agglomeration grows until gravitational forces overcome drag forces and the agglomeration precipitates.

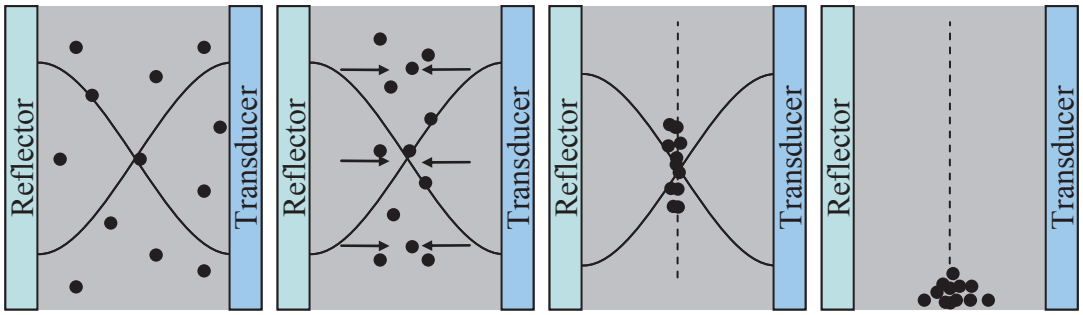

Figure 1.5 Enhanced sedimentation of particles with a density greater than the fluid using ultrasonic concentration

This technique has been reported in literature by Gaida et al. (1996) with the commercial development of a flow-through macro-scale mode. An inlet was added at the bottom of the resonator and flow was allowed through one side vertically through the field. A clarified outlet was located at the top and a particulate output was placed below the resonator under the inlet. Hawkes and Coakley (1996) built a smaller device designed to have a small volume for the concentration of yeast cells. When applied to bacterial cells the system was not as successful. This was due to the Stokes drag forces which dominate for smaller particles. Sedimentation is only useful for relatively high concentration of particles because it depends on many cells aggregates and falling out of suspension.

1.7.2 Cell Washing

The cell washing technique bas been demonstrated to work effectively with polyamide spheres, yeast (Hawkes et al. 2004), and also bovine red blood cells (Petersson et al. 2005). Figure 1.6 shows a schematic representation of the microfluidic device used by Petersson et al. (2005) which consisted of two fluid streams flowing in the same direction; one fluid stream, "A," is the clean fluid and fluid stream "B" is the fluid with particles that were moved over into fluid "A" without disturbing or intermixing of the two fluid streams. Hawkes et al. reported being able to wash 80% of the yeast particles into fluid "A," while Petersson et al. reported a 98% exchange of red blood cells washed into clean plasma.

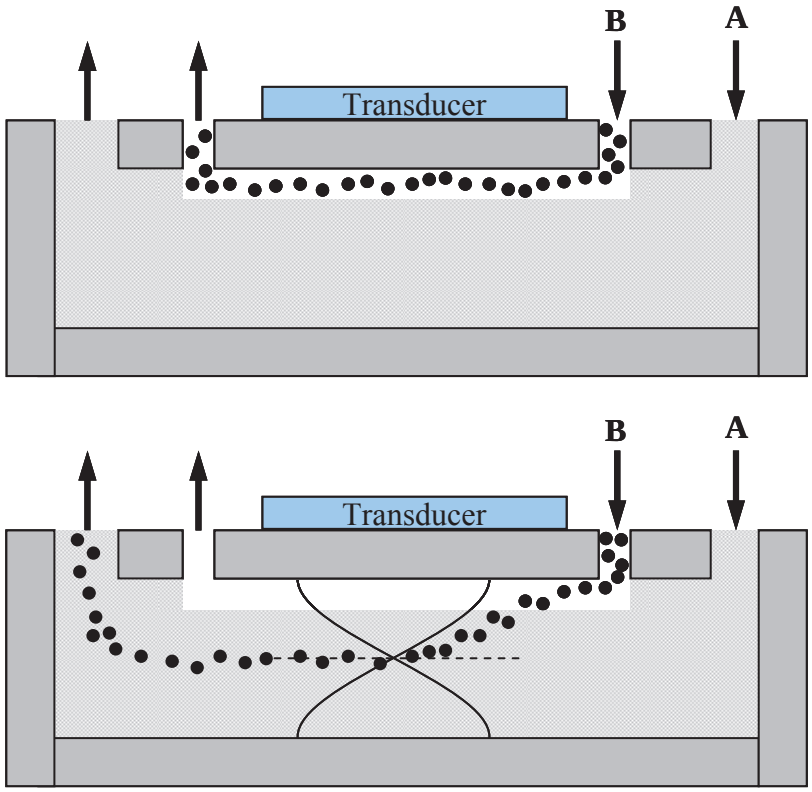

Figure 1.6 The principle of cell washing using ultrasonic forces

1.7.3 Size Fractionation

The fractionation of different sized cells as shown in Figure 1.7 visually describes how the larger particles experience more force in the quarter-wave standing-wave chamber. The difference in how far up the particles are forced is dependent on the

acoustic radiation force and the radius of the particle (under the assumption the *acoustic contrast factor* are the same for both particles). Aboobaker et al. (2003) made the prediction of fractionating different sized particles based off there size, acoustic radiation forces, and also the particles terminal velocity in the fluid.

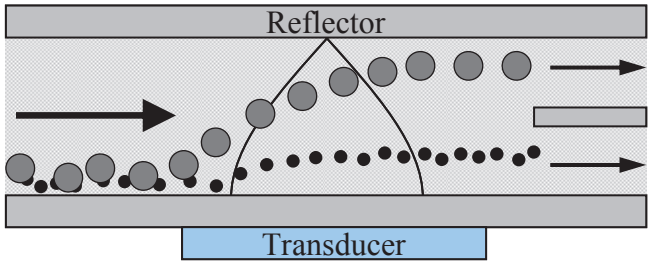

Figure 1.7 Principle of fractionation using ultrasonic forces.

1.7.4 Laminar Flow Filtration

Flow-through filtration uses acoustic radiation forces to draw particles within a part of a channel's cross section, and then draws them out from a concentrated outlet while the remaining fluid exits from a clarified outlet. This technique was tested by Hawkes and Coakley (2001) by using a 250 μm deep channel made from stainless steel and driven at 3MHz. Latex particles between 1.5 and 25 μm and also yeast cells were tested in the system; they achieved clarification of up to 1,000-fold.

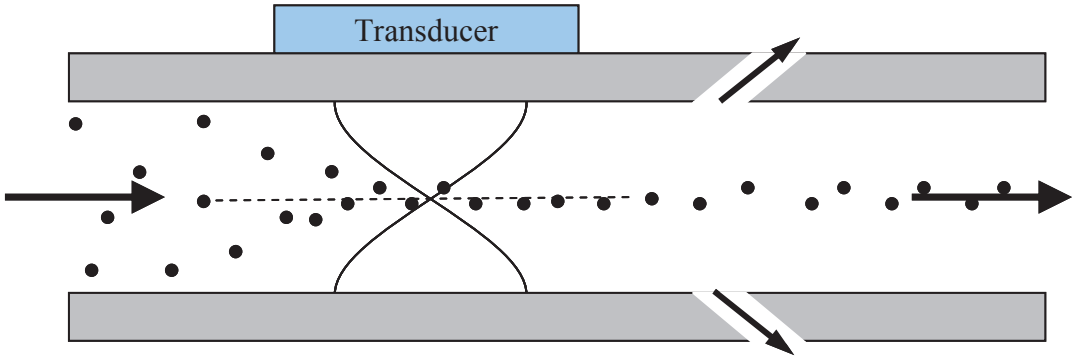

Figure 1.8 Laminar flow filtration using ultrasonic forces

Harris et al. (2003) designed a micro flow through filter which used channels etched into a Pyrex and silicon structure. The device achieved a 50-fold clarification of yeast cells. However, only a 5-fold clarification was seen for 1 μm particles. Petersson et al. (2004) designed a device to filter lipid particles from whole blood. Red blood cells in plasma move to pressure nodes while lipids move to pressure antinodes; red cells get

concentrated in the center of the channel. The channels were 350 μm wide and etched into silicon, and the transducer was orthogonal to the direction of the standing wave such that several channels could be excited from a single transducer. More than 70% of the red cells were collected in one third of the fluid volume while more than 80% of lipid particles were removed.

1.7.5 Filtration Using Ultrasound Within a Porous Mesh

Another alternative to filtration techniques is to use radiation forces within an ultrasonic field to modify filtration characteristics of a porous mesh (Grossner et al., 2005). A filter can be created when the mesh is excited ultrasonically causing the acoustic radiation forces to hold particles on the mesh (of pore size up to two magnitudes larger than the particles). In order to release the particles, the ultrasonic signal is turned off. A more successful attempt at concentrating micro particles was done by Wang et al. (2004) using a polymer mesh; they achieved with the up to 90% particle retention and also a maximum of 1.5×10^8 cells mL^{-1}.

1.8 Proven Design Concepts

A system employing the basic principles of a typical standing wave field, described above, was built by Danao (2005). A Parallel Disc ultrasonic chamber using cylindrical tubes with piezoceramic discs was fabricated which was shown to force 7μm polystyrene beads along the nodal planes.

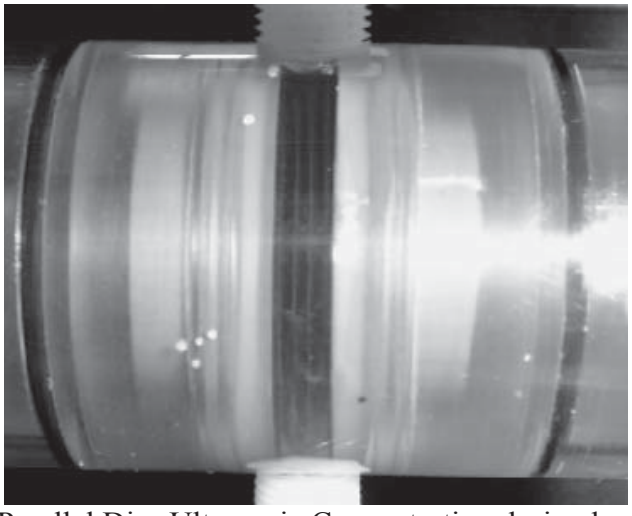

Figure 1.9 Photo of Parallel Disc Ultrasonic Concentration design by Grace Danao

Wang et al. at Cleveland State University and Case Western Reserve University built another system for concentrating biological cells. Their design used a reticulated polyurethane mesh between the piezoceramic discs which helped to trap particles as the liquid media flowed through the mesh thus concentrating the polystyrene beads and also mouse hybridoma cells when the ultrasonic field was released.

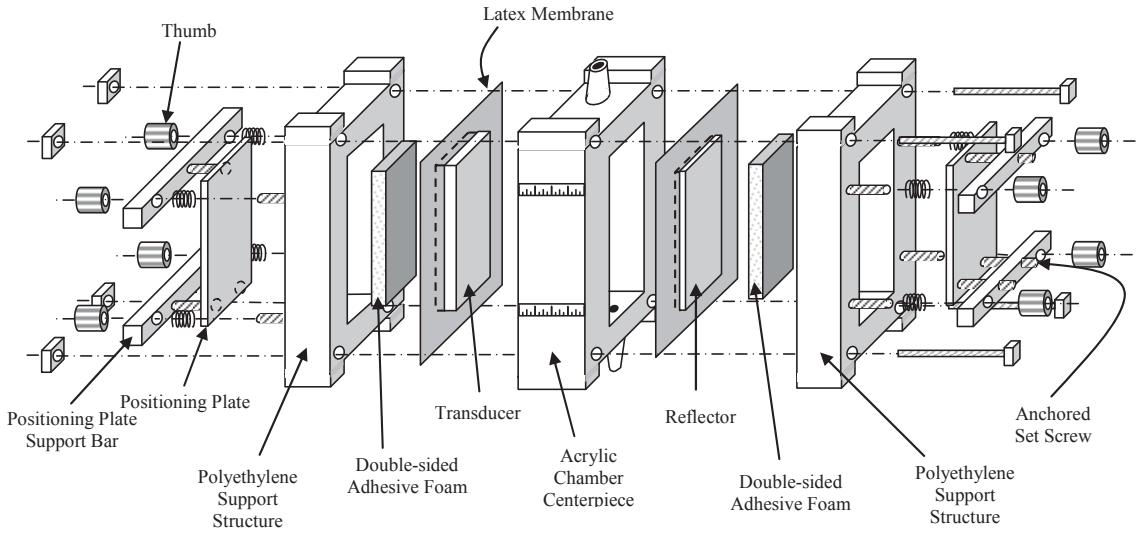

Figure 1.10 Diagram of the design used in Wang et al., 2004.

1.9 Ultrasonic Forces on Particles

The forces exerted on particles in an ultrasonic standing field are dependent on both the density difference with the medium and also the volume of the particle of interest; as the density difference increases and the volume of the particle increases, then so do the forces acting on that particle.

The particles in question in this research are 10μm polystyrene beads, 5-10μm *S. cerevisiae* yeast cells, and also rod-shaped *E. coli* bacteria cells with an average size of 0.5μm diameter by 1μm long.

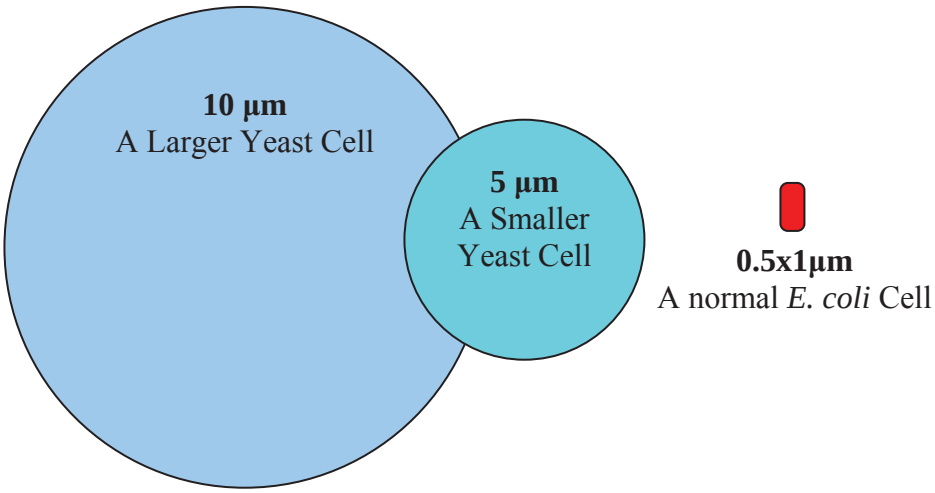

Figure 1.11 Scaled view *S. cerevisiae* yeast cells and an *E. coli* bacterium.

1.9.1 Gravity, Density Difference, and Buoyancy

The most common forces on a particle we are familiar with and are considered common sense. If you put a pebble in water, it sinks; if you put a piece of wood in water, it floats. Although gravity is pulling down on everything, the specific gravity for most woods are less than one, which means they are pushed to the surface of the denser liquid medium. Yeast and bacteria both have a density close to1.1 g mL^{-1}; 1.113 g mL^{-1} for *S. cerevisiae* (Baldwin and Kubitschek, 1984) and 1.105 g mL^{-1} for *E. coli* (Martinez-Salas et. al., 1981). With densities greater than water (1.000 g mL^{-1} at 25°C), both yeast and *E. coli* are negatively buoyant.

$$\text{Buoyancy} = F_B = \frac{4}{3}\pi R^3 g\left(\rho_f - \rho_p\right) \qquad 1.2$$

Where R is the particle's radius, g is gravity, ρ_f is the density of the fluid, and ρ_p is the density of the particle.

1.9.2 Fluid Drag Force

Stokes equation of drag force on a spherical particle in a fluid flow is given as:

$$F_{Drag} = -6\pi\mu R v \qquad 1.3$$

Where "v" is the average fluid velocity, R is the radius of the particle, µ is the dynamic viscosity of the fluid (0.001 $kgm^{-1}s^{-1}$ for water). It should be noted that fluid velocity (v)

is a linear term; changing fluid velocity influences the drag force linearly with radius ® and dynamic viscosity.

1.9.3 Acoustic Radiation Force

King (1934) derived the first mathematical equation to characterize the acoustic radiation force on small particles within a ultrasonic standing wave, however his work was based on rigid, non-compressible sphere and also an invisid fluid. Yosioka and Kawasima (1955) expanded on King's equations and included something called the *acoustic contrast factor* to account for the compressibility of bubbles and other compressible spheres. Yosioka and Kawasima's equation is shown in Equation 1.4.

$$F_{ac}(x) = 4\pi k E_{ac} R^3 \Phi(\beta,\rho)\sin(2kx) \qquad 1.4$$

Where x is the distance along the direction of applied acoustic energy, k is the wave number $(k = 2\pi/\lambda)$, λ is the wavelength, E_{ac} is the acoustic energy density (see Equation 1.6), and $\Phi(\beta,\rho)$ is the *acoustic contrast factor* expressed in Equation 1.5.

$$\Phi(\beta,\rho) = \frac{\rho_p + \frac{2}{3}(\rho_p - \rho_w)}{2\rho_p + \rho_w} - \frac{\beta_p}{3\beta_w} \qquad 1.5$$

Where ρ_p and ρ_w are the densities of the particle and the water, respectively and β_p and β_w are the compressibilities of the particle and water, respectively.

The *acoustic energy density*, E_{ac}, is expressed in Equation 1.6.

$$E_{ac} = \frac{P_{ac}}{(A)(c)} \qquad 1.6$$

Where P_{ac} is the *acoustic power* and A is the area by which the energy is applied and c is the speed of sound of the medium the acoustic energy is entering.

Additionally, it is worth noting that the *sound pressure* is calculated as the square root of the *acoustic power* multiplied by the medium's acoustic impedance divided by the area of sound propagation as shown in Equation 1.7

$$p = \sqrt{\frac{P_{ac} Z}{A}} \tag{1.7}$$

Where Z, or the acoustic impedance is equal to the density times the speed of sound of the material, $Z=\rho c$.

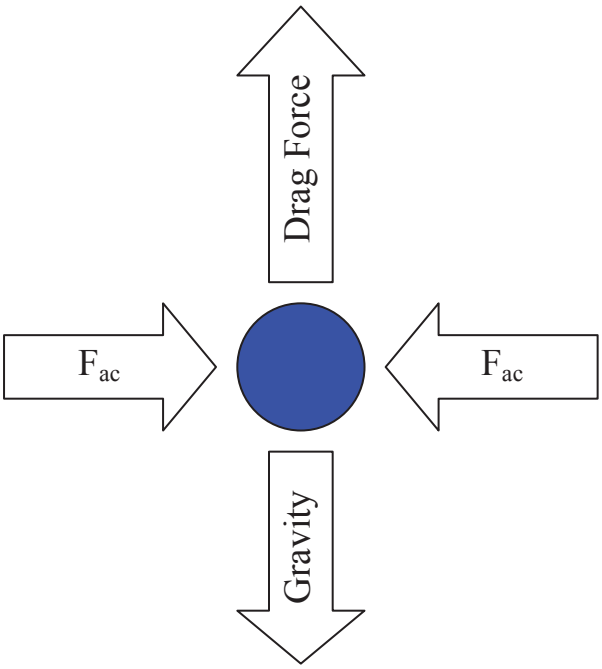

Figure 1.12 Forces acting on a micro particle under an ultrasonic standing wave.

CHAPTER 2 : OBJECTIVE

The goal of this research is to enhance the detection limits of microorganisms by developing a system to concentrate microorganisms in a liquid medium. The specific objectives were to:

Design a system for concentrating microorganisms using ultrasonic concentration.

Determine the effects of frequency, flow rate, initial concentration, volume throughput, voltage application, and polyurethane foam pore density on efficiency of the system for concentrating yeast.

Determine the effects of frequency, flow rate, initial concentration, volume throughput, voltage application, and polyurethane foam pore density on efficiency of the system for concentrating bacteria.

CHAPTER 3 : MATERIALS AND METHODS

3.1 Overview of the Laboratory Setup

Testing was performed with a combination of using the prototype chamber, the Optical Density Detector, a syringe pump, function generator, power amplifier, oscilloscope, DAQ board, and laptop for data collection. A one-way factorial design with three or four treatments levels, three replications and with the order of the treatment randomized was selected for testing the effects of power, frequency, flow rate, volume throughput, foam density, and concentration. The laboratory apparatus is shown in Figure 3.1.

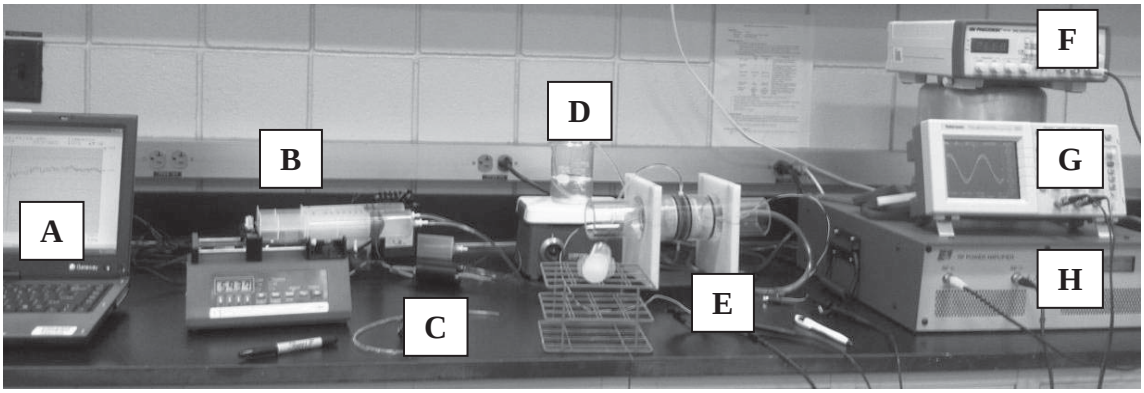

Figure 3.1 Laboratory testing setup, from left to right: laptop for data acquisition (A); syringe pump for continuous laminar flow (B); Optical Density Detector (C); hard to see because it is black on a black tabletop); beaker of yeast suspension on top of a motorized magnetic stirrer (D); assembled ultrasonic concentration prototype (E); Function generator (F); Oscilloscope (G); Power Amplifier (H).

3.2 Selection of Yeast

A particular strain of yeast was acquired based on its non-flocculating behavior. A non flocculating behavior was desired to prevent clumping in the ultrasonic chamber. Clumping would create a biased result because the plate counts would not reflect the actual concentration and the optical density would be erroneous. The yeast (strain #1007, WY 1007) was obtained from Wyeast Labs Inc. Odell, Oregon. The yeast was grown using a 0.1% Potato Dextrose Broth (PDB) solution.

3.3 Selection of *E. coli*

The strain of *E. coli* used in this experiment was a nonpathogenic strain *E. coli* K12 (ATCC 11775) and was obtained from the Department of Food and Animal Sciences, University of Kentucky. The bacteria were stored on a slant of Brain Heart Infusion agar (BHIA) [BD Diagnostics, Franklin Lakes, NJ] and inoculated from the slant to a 250 mL bottle of Brain Heart Infusion broth (BHI) [BD Diagnostics, Franklin Lakes, NJ] the day before experimentation.

3.4 Enumeration of Microorganisms

A measurement of particulate concentration was needed to characterize the dynamic changes and measure the performance of the Ultrasonic Concentration prototype. An Optical Density Detector was constructed from black acetyl resin (Delrin). The transmission path length was 51 mm with a diameter of 6.35 mm. See Figure 3.2, Figure 3.3, and also Appendix A on page 62 for more information. A 627 nm LED was installed behind a window in one end and a TAOS TSL 257 detector behind a window on the other end. The current to the LED was adjusted such that the detector voltage was 1.5 V with clear water. This device was calibrated with yeast and microbial concentration fluids as described later. A Data Acquisition (DAQ) board (Measurement Computing USB-1408FS) was used to convert, read and record the voltage signals from the Optical Density Detector.

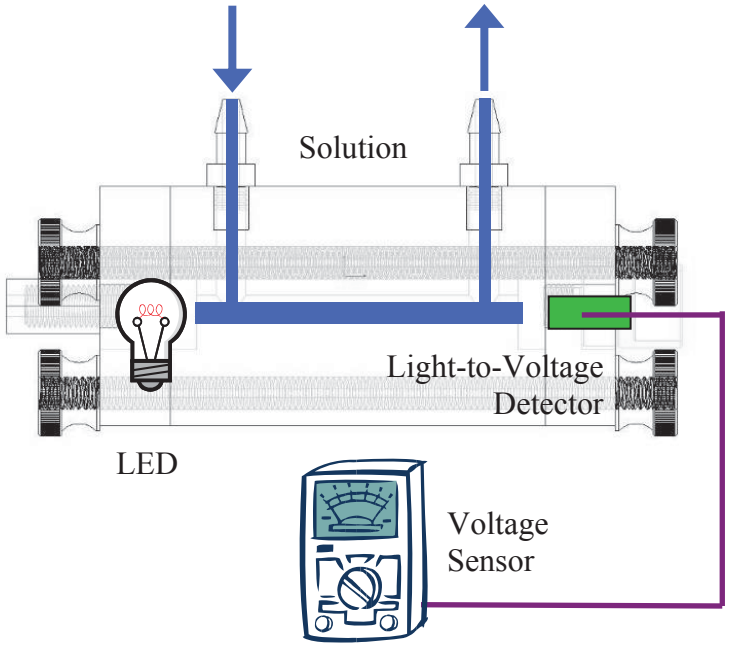

Figure 3.2 Optical Density Detector schematic for continuous measurement of outflow

The completed Optical Density Detector used can be seen in Figure 3.3.

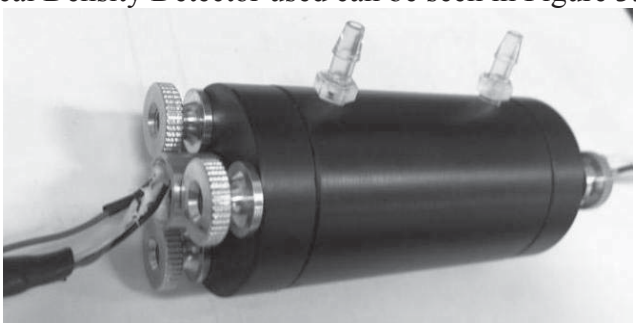

Figure 3.3 Picture of the Optical Density Detector

3.5 Laboratory Setup

A laboratory system was developed to test the system designed using two piezoceramic discs held in a parallel confiuration with three concentric tubes; two smaller tubes (1.5" OD x 2" ID) to hold the piezoceramics and one larger diameter tube (3" OD x 2-5/8" ID) to hold the smaller tubes. Clear acrylic tubing was used to construct the chamber and disc holders. Clear plastic was used for visibility, non-conductive, and easy machining properties.

The piezoceramic discs chosen were the thickest and largest diameter that could be found commercially available. The discs were manufactured by Steiner and Martins

Inc. and were 43 mm in dimeter and 10.5 mm thick (see Appendix C on page 68 for more information). The piezoceramic discs were arranged in a parallel configuration with an approximate 12 mm distance between discs to create a acoustic chamber as shown in Figure 3.4. See Appendix B on page 65 for mechanical drawings.

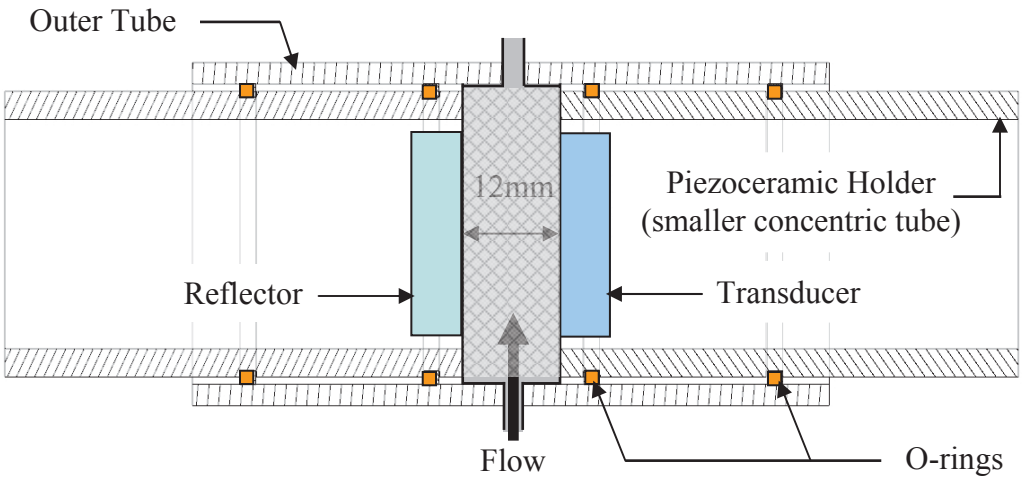

Figure 3.4 Cross sectional view of the parallel disc ultrasonic concentration prototype

The electrical equipment used in the laboratory setup was a sinusoidal signal generator (BK Precision 4012A 5MHz Sweep/Function Generator, Yorba Linda, CA) which sent a low voltage signal to a power amplifier (E&I 2100L RF Power Amplifier; 100W, Class A; 10 kHz – 12 MHz, 50dB Gain, Rochester, NY). The power amplifier increased the voltage being applied to the piezoceramics and also dissipated the reflected power.

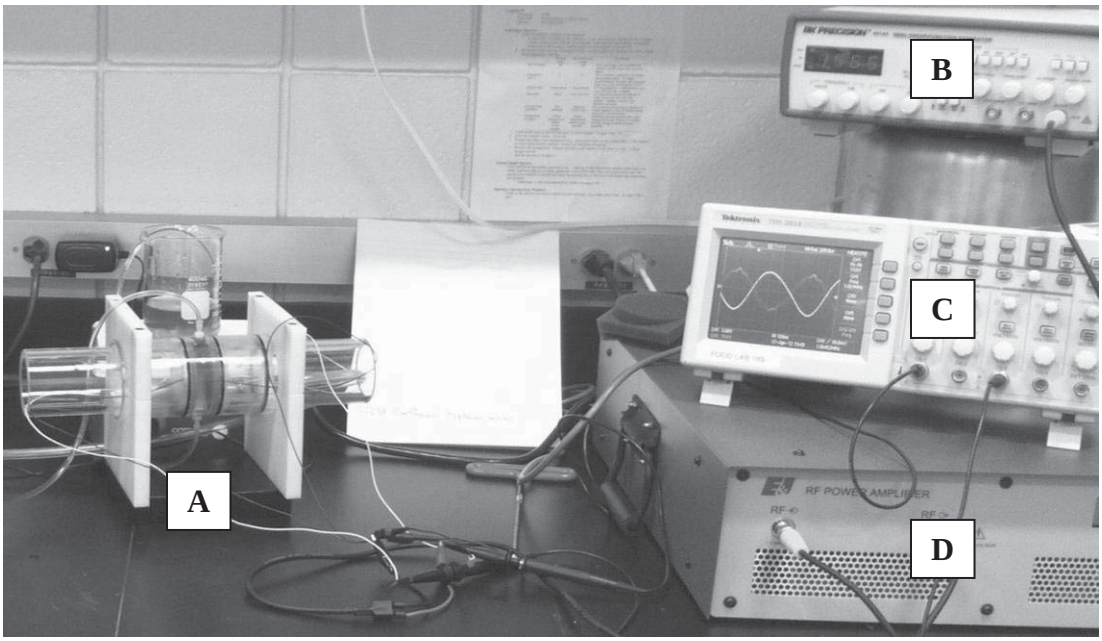

Figure 3.5 Ultrasonic Concentration system developed for concentrating microparticles showing the Ultrasonic Concentration prototype A; the BK precision Sweep Generator, B; the Tektronix oscilloscope, C; and the E&I power amplifier, D.

The ultrasonic waves induced by the voltage signal traveled through the water path which was typically 1.2 cm and was then reflected off an opposing piezoceramic. The reflected signal generated a similar signal to the power signal. Both power and reflected voltage signals were viewed on an oscilloscope (Tektronix TDS 2012: Two Channel Digital Storage Oscilloscope; 100 MHz 1GS/s). The frequency of the power signal was thus adjusted to achieve a maximum rebounding/reflecting signal. This technique allowed the chamber and piezoelectric transducers to be adjusted to resonance. At ultrasonic resonance there were standing ultrasonic wave in the chamber with nodal planes for the micro particles to move towards.

The fluid system used syringe pumps to maintain an accurately variable yet non-pulsatile laminar flow to the ultrasonic chamber (New Era Pump Systems; NE-4000 & NE-1000 Programmable Syringe Pumps). The performance range of the syringe pumps could continuously vary output flow between 0.1 and 1,000 mL min^{-1} and could accept syringes as large as 140 mL.

3.6 Experimental Design

The test design was to determine to performance of the system for both yeast and bacterial concentration. The first vegetative cell chosen to evaluate in the Ultrasonic Concentration prototype was yeast because of it relatively large size (5-10μm), widespread availability, ease of growth, and non-virulence. The primary variables considered to affect ultrasonic separation included initial sample concentrations, frequencies, flow rates, foam densities, voltages, and also volume throughputs and duty cycles of the applied voltage.

3.6.1 Initial Concentration

Different concentrations of the initial yeast sample was a variable because the system could work better at a stronger or weaker concentration, and possibly get saturated and not work well at all at the higher initial yeast concentrations. Three levels were chosen 100,000 cells mL^{-1}; 500,000 cells mL^{-1}, and 1,400,000 cells mL^{-1} that resulted in voltage outputs from the Optical Density Detector of 1.3, 0.9, and 0.3 V, respectively. These concentrations were within the exponentially linear detection limits of the Optical Density Detector (see the calibration curve, Figure 3.11, page 28). Initial concentration testing was not performed with the bacteria because the range in concentrations able to be distinguished from the Optical Density Detector was within one log cycle (0.5×10^7 to 5.0×10^7 CFU mL^{-1}). Based off previous research done by Cousins et al. 2001, Gupta and Feke 1997, and Hakes and Coakley 1996, the effect of concentration changed when going from 10^7 to 10^9 cells mL^{-1}, concentrations within one log-cycle were not tested. Therefore, based off the non-significant effect of initial concentration from the previously completed yeast experimentation, testing the initial concentration of bacteria effect on concentration efficiency was not performed.

3.6.2 Frequencies

There were several resonant frequencies discovered under initial testing, and determination of the optimal frequencies. It was believed that a higher frequency (smaller wavelength) would provide a smaller distance for the microorganisms to travel to a nodal plane. The frequencies chosen for testing were 667 kHz, 1113 kHz, 1560 kHz,

2456 kHz, and 2900 kHz. Frequencies above 2900 kHz were found to produce noise within the electronics and were not tested.

3.6.3 Flow Rate

The flow rate of the system was determined to be an important variable because the only force holding the micro-particles in the chamber was the ultrasonic pressure force. The higher the flow rate, the greater the drag forces were pulling the particle out of the chamber. While at the lower the flow rate, a greater amount of time was required for sampling and that led to an increased temperature in the chamber cell. The flow rates chosen were 4 mL min^{-1}; 8 mL min^{-1}; 16 mL min^{-1}; 32 mL min^{-1} based on research done by Wang et al., 2004.

3.6.4 Foam Density

The density or porosity of the reticulated polyurethane foam was thought to be an important consideration in the experimental testing because a smaller pore size could enhance the retention of micro particles and also create a more tortuous path for the particles to flow out from being trapped by the ultrasonic pressure forces. The foam densities chosen were 45, 60, and 100 pores per inch (PPI). It was believed that pore sizes lower than 45 PPI would be too "open" and pore sizes greater than 100 PPI would impede flow through the reticulated foam and consequently the entire volume of the chamber would not be utilized. Figure 3.6 shows different foam densities that were cut to a diameter (66.7 mm) and thickness (12 mm) to fit between the parallel piezoceramic discs shown in Figure 3.4.

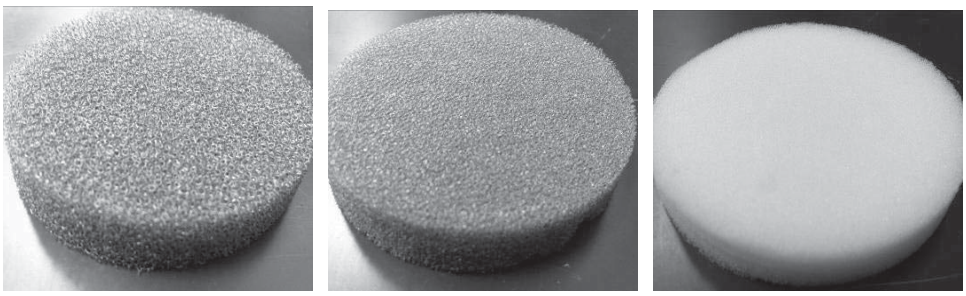

Figure 3.6 Different foam densities 45, 60, and 100 PPI from left to right.

3.6.5 Voltage Duty Cycle

The nature of the system was to use an ON/OFF cycling of the ultrasonic waves. This method would trap particles in the chamber while the power amplifier was on and

then release them after the chamber was saturated with particles and exude a concentrated slurry of particles. The volumes with applied voltage chosen for experimentation were 50 mL, 100 mL, and 200 mL. The maximum volume of 200 mL was based on the allowable limits of the using two syringe pumps and a total of three 140 mL syringes which needed additional volume collection before and after voltage was applied and then discontinued to the piezoceramic. The syringe pumps used were both New Era Pumps, Farmingdale, NY. The NE-4000 model had space for two syringes, and the NE-1000 space for one syringe; both capable of a maximum syringe size being 100 mL.

3.6.6 Voltage Amplitude

Ultrasonic concentration relies on the pressure forces induced into the liquid medium; increasing voltage input to the piezoelectric transducers increases the mechanical displacement; theoretically creating higher pressures, increased acoustic radiation forces, and furthermore a larger force holding particles that results in a greater concentration. However, there is a tradeoff between cell viability and bursting cells and also creating waste heat in the chamber and killing cells. The voltage amplitudes chosen were a balance between the limits of creating excess heat and having sufficient mechanical displacement for a noticeable signal difference. Voltages levels selected for testing were 1000VAC, 1500VAC, and 2000VAC.

3.7 Separation of yeast and bacteria for experimentation

The initial culture of yeast was grown daily in a smaller 250 mL vessel to ensure that the yeast samples were in a similar growth phase when tested. Daily cultures were put into four 50 mL centrifuge tubes and spun at 2500 revolutions per minute (rpm) for 5 minutes to collect the yeast cells. Figure 3.7 shows the separated yeast in the bottom of a centrifuge tube.

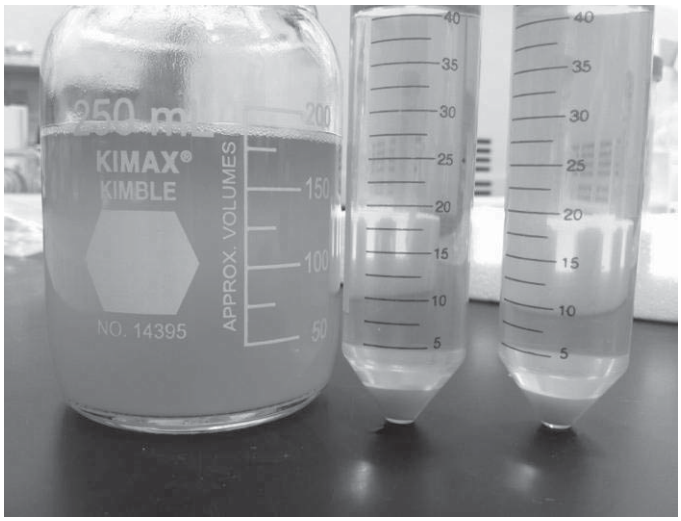

Figure 3.7 Left shows the daily culture of 250 mL of yeast. The right two tubes show a centrifuged sample of the daily culture into 50mL centrifuge tubes.

The growth media was discarded, and the samples were washed by re-suspension in Sodium Polyphosphate (SP) [Spectrum Chemical, Gardena, CA] and Peptone Water (PW) [BD Diagnostics, Franklin Lakes, NJ] which were mixed together to form (SP+PW) with concentrations of 0.1 and 1.0 g L^{-1}, respectively. The SP+PW solution was a standard media for microorganism recovery (Hill V. R. et al., 2004). The samples were then re-centrifuged and re-suspended in solutions used for experimentation.

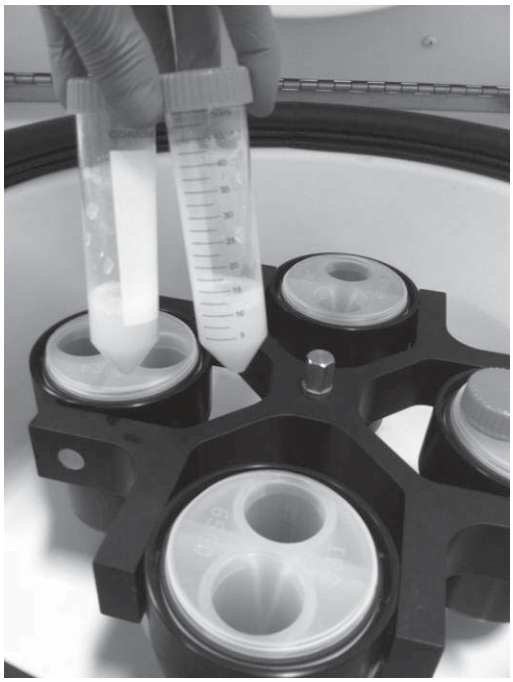

Figure 3.8 Left shows re-suspended yeast sample before centrifugation. Right shows the washed yeast sample after centrifugation

Similarly for *E. coli*, the cultured suspension was separated into two centrifuge tubes, spun in the centrifuge at 3000 rpm for 5 minutes, the media supernatant was discarded, the pellet was re-suspended in SP+PW, re-centrifuged, decanted again, and finally re-suspended.

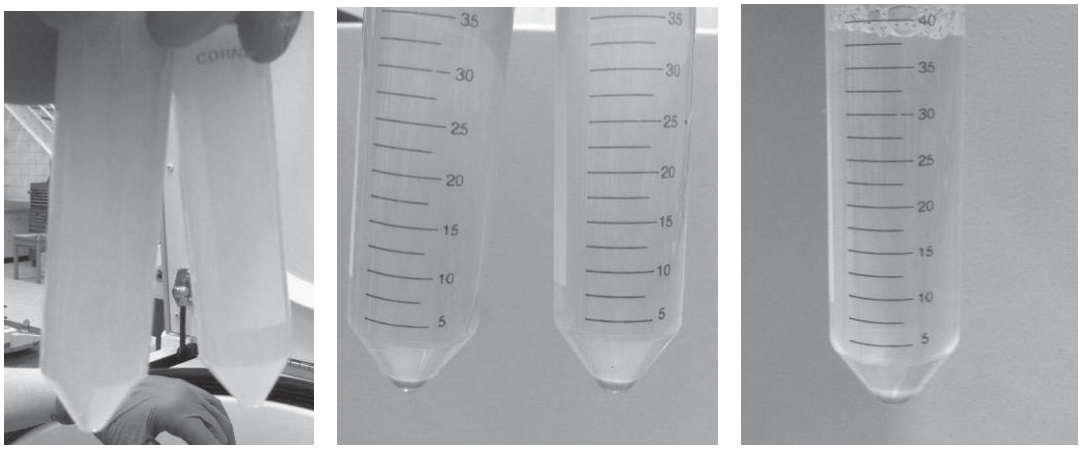

Figure 3.9 Pictures of *E. coli* suspension before, during, and after centrifugation and washing procedure.

Next, the concentrated suspension of extracted yeast or bacteria was diluted into the desired initial concentrations for experimentation, between 1.0×10^5 and 1.5×10^6 cells mL^{-1} for *S. cerevisiae* and between 1.0×10^7 and 2.0×10^7 cells mL^{-1}.

Figure 3.10 Dilute samples of yeast in SP+PW used in experimentation.

3.8 Calibration of the Optical Density Detector

Various suspensions of yeast with concentrations from 2,000 to 2,500,000 cells mL^{-1} were pumped through the optical device and the voltage output recorded. The suspensions were then collected and plated on 3M™ Petrifilm™ for yeast (Catalog # 6407 and 6417). The plate count of yeast and voltages are plotted in Figure 3.11.

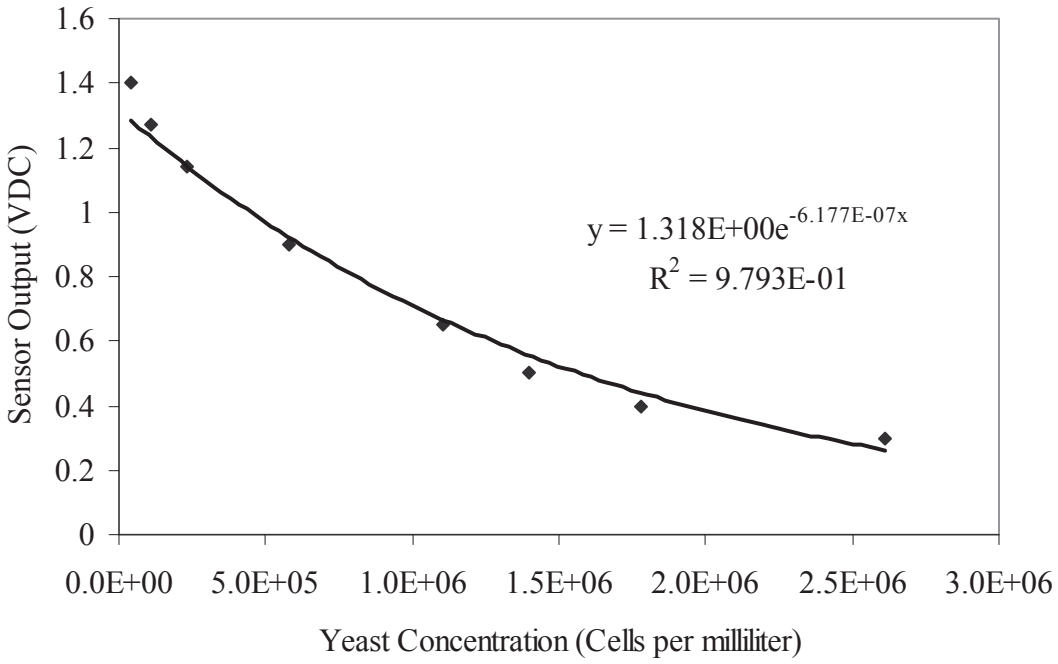

Figure 3.11 Plot of Yeast Calibration curve for various dilutions of yeast

Microsoft Excel was used to find a line of best fit and the equation given was:

$$\text{Voltage} = 1.318e^{-1.853E-5*\text{concentration}} \quad 3.1$$

Thus the reverse equation for determining yeast concentration from voltage was calculated in Equation 3.2

$$\text{Concentration} = \left(\frac{\ln\left(\frac{\text{Voltage}}{1.318} \right)}{-1.853\text{x}10^{-5}} \right) \quad 3.2$$

3.8.1 Calibration of *E. coli*

Similar to the calibration of yeast, the calibration of the Optical Density Detector for *E. coli* bacteria used various suspensions with bacterial concentrations from 100,000 to 50,000,000 cells mL^{-1} were pumped through the optical device and the voltage output

recorded. The suspensions were then collected and plated on 3M™ Petrifilm™ for bacteria (Catalog # 6404 and 6414). The plate count of bacteria and voltages are plotted in Figure 3.12.

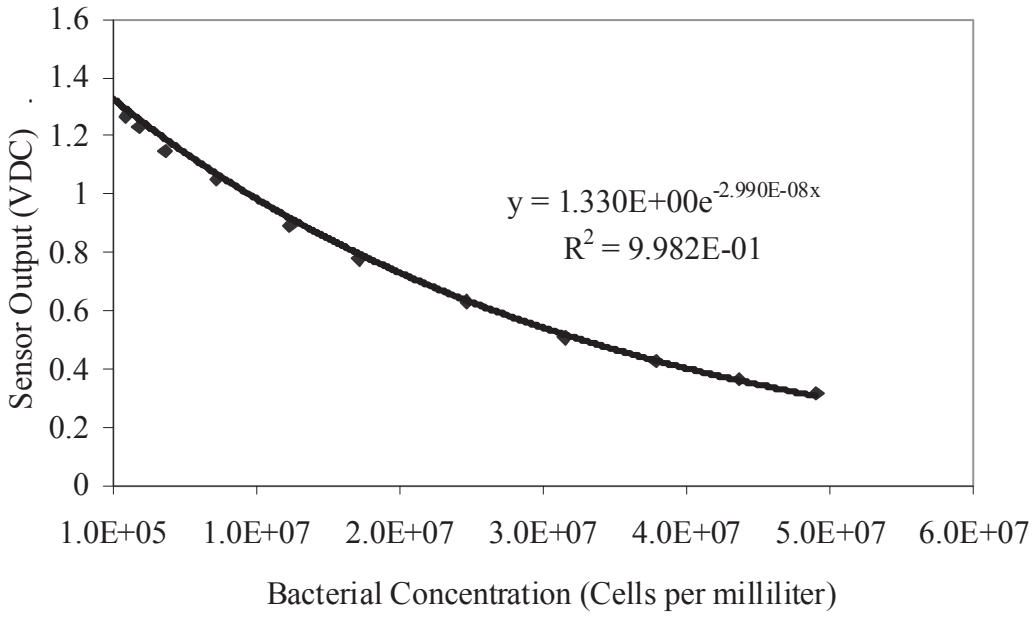

Figure 3.12 Plot of *E. coli* calibration curve for various dilutions of *E. coli*.

The equation for detecting yeast was calculated by Microsoft Excel in Equation 3.3

$$\text{Voltage} = 1.333e^{-2.990E-8*\text{concentration}} \tag{3.3}$$

Thus the reverse equation for determining yeast concentration from voltage was calculated in Equation 3.4.

$$\text{Concentration} = \left(\frac{\ln\left(\frac{\text{Voltage}}{1.330} \right)}{-2.990\text{x}10^{-8}} \right) \tag{3.4}$$

CHAPTER 4 : RESULTS

4.1 Validation of the System Performance Using Polystyrene Beads

The Ultrasonic Concentration system was tested for concentration of 10μm polystyrene spheres to verify the system performance. Then *S. cerevisiae* yeast cells were tested to show that the system would work with vegetative cells that had a density only slightly different than water. Then the prototype was tested with *E. coli.*

Figure 4.1 Close-up view of concentrated red 10μm polystyrene particles (shown without reticulated mesh)

4.2 Concentration Measurements

A typical response of the optical concentration detector as measured during a test cycle is shown in Figure 4.2. The starting voltage (or "start" in the following tables) is the voltage given by the initial concentration of yeast. After the power amplifier was turned on, the yeast were trapped in the chamber, hence, the Clarified Voltage ("clear" in the following tables) was a higher voltage because there was less yeast in the output stream of the Ultrasonic Concentration prototype. Finally, the power amplifier was turned off – the yeast were no longer being held in the chamber by the ultrasonic forces and were released from the chamber – the increased concentration of yeast from the chamber blocked the light to the voltage detector and a decreased voltage was detected for the Concentrated Voltage (or "Conc." in the following tables).

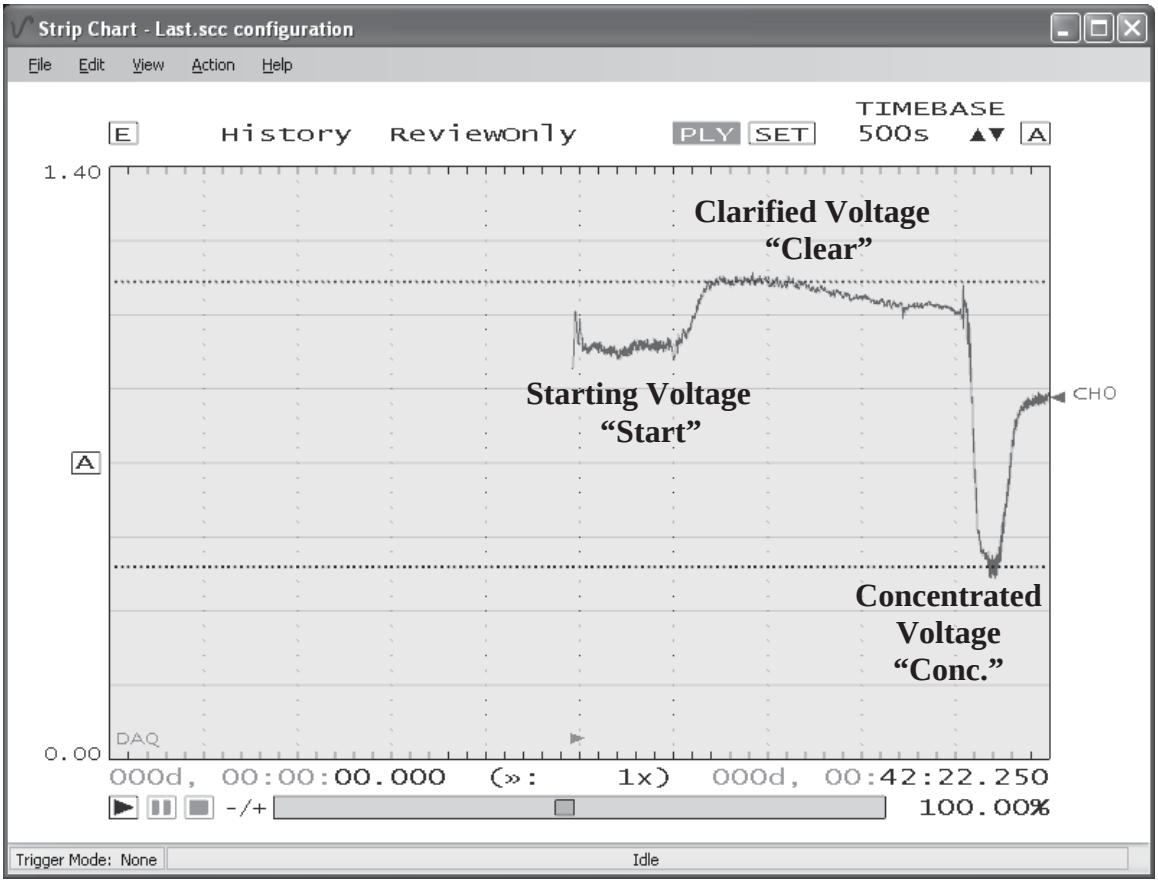

Figure 4.2 Screen capture from the laptop data acquisition software.

4.3 Initial Concentration Testing with *S. cerevisiae*

This test was conducted to determine if there was an effect on concentration efficiency with relation to initial concentrations of yeast. Three concentrations of yeast were chosen for testing based on their voltages: 100,000 cells mL^{-1} (1.3V); 500,000 cells mL^{-1} (0.9V); and 1,400,000 cells mL^{-1} (0.5V). The concentrations were chosen based on the upper and lower limits of the Optical Density Detector's ability to measure a significant signal from the yeast suspensions.

The testing was completed with the following testing conditions: the frequency was maintained around 1560 kHz and adjusted to maintain resonance; the voltage input was maintained at 1000 VAC peak-to-peak; and the flow rate was maintained at 16 mL min^{-1}.

The testing procedure was to take a baseline signal from 60mL to collect a starting voltage, activate the power amplifier for 100 mL with 1000 VAC to collect a clear detector voltage, deactivate the power amplifier and collect 40 mL of the concentrated portion. The "Start", "Clear" and "Conc" voltages from the Optical Density Detector are provided in Figure 4.2. The results for the factorial test of the effect of initial yeast concentration are shown in Table 4.1

The yeast cell concentrations were calculated based on the calibration curve and the measured Detector Voltage. Percent Clarified was calculated by taking the difference between the Baseline and Clarified concentrations divided by the Baseline concentration.

$$\text{Percent Clarified} = \frac{[\text{Baseline}] - [\text{Clarified}]}{[\text{Baseline}]} \text{x}100 \qquad 4.1$$

The Percent Concentrated was calculated by taking the difference between the Baseline and Concentrated concentrations divided by the baseline concentration.

$$\text{Percent Concentrated} = \frac{[\text{Concentrated}] - [\text{Baseline}]}{[\text{Baseline}]} \text{x}100 \qquad 4.2$$

Table 4.1 Initial Concentration (Low: 30,000 cell mL^{-1}; Medium: 90,000 cells mL^{-1}; High: 200,000 cells mL^{-1}) testing results with *S. cerevisiae*

	Detector Voltage			Concentration (cfu mL^{-1})				
Low	Start	Clear	Conc.	Start	Clear	Conc.	Percent Clarified	Percent Conc.
Rep # 1	1.207	1.250	1.010	41,895	36,384	69,947	13%	67%
Rep # 2	1.343	1.400	1.267	25,086	18,543	34,257	26%	37%
Rep # 3	1.377	1.437	1.295	21,151	14,436	30,816	32%	46%
Rep # 4	1.309	1.377	1.241	29,123	21,151	37,522	27%	29%
Average				29,314	22,628	43,136	25%	45%
Medium								
Rep # 1	0.901	1.003	0.697	87,926	71,042	128,341	19%	46%
Rep # 2	0.861	0.986	0.723	95,075	73,733	122,685	22%	29%
Rep # 3	0.879	0.995	0.740	91,818	72,303	118,917	21%	30%
Average				91,606	72,359	123,314	22%	29%
High								
Rep # 1	0.425	0.545	0.390	206,222	167,069	219,752	19%	7%
Rep # 2	0.560	0.620	0.320	162,795	146,771	250,896	10%	54%
Rep # 3	0.501	0.620	0.360	180,322	146,771	232,353	19%	29%
Rep # 4	0.450	0.553	0.298	197,223	164,918	262,373	16%	33%
Average				186,641	156,382	241,344	16%	31%

The average measured concentrations tested were 30,000, 90,000, and 200,000 cells mL^{-1}. The percent clarification ranged between 10% and 32%. Likewise, the percent concentration ranged between 7% and 67%. The data were plotted in Figure 4.3 and there appeared to be no slope correlation. An ANOVA was conducted with results as shown in Table 4.2 and no significant difference was found.

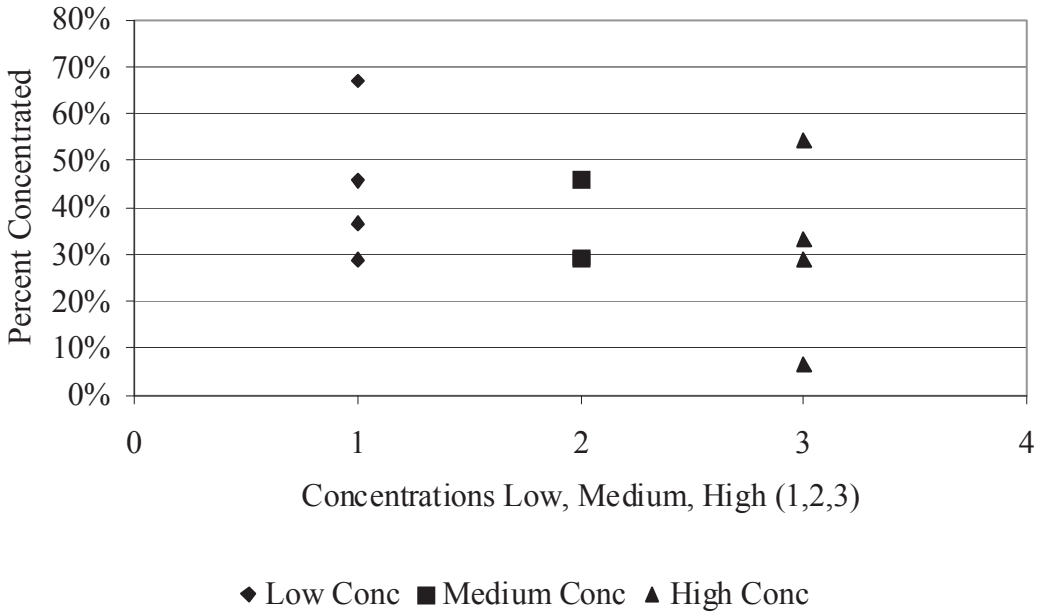

Figure 4.3 Initial Concentration effect on the concentration of *S. cerevisiae*

Table 4.2 Initial Concentration effect on the concentration of *S. cerevisiae* ANOVA

Groups	Count	Sum	Average	Variance
LowConc	4	0.1414	0.0353	0.0001
MediumConc	3	0.0781	0.026	4E-05
HighConc	4	0.0856	0.0214	0.0002

ANOVA

SourceofVariation	SS	df	MS	F	P-value	Fcrit
BetweenGroups	0.0004	2	0.0002	1.8532	0.2181	4.459
WithinGroups	0.0009	8	0.0001			
Total	0.0013	10				

4.4 Initial Concentration Testing with *E. coli*.

Since the results for the yeast concentration testing were not statistically significant and the fact that the useable range of the Optical Density Detector was within one log-cycle of concentration, it was determined that testing three different concentrations in one log-cycle would not provide any useful information, and concentration testing was not performed for *E. coli* cells.

4.5 Resonant Frequency Testing with *S. cerevisiae*

Four frequencies were tested based on the resonance with the piezoceramic discs and the chamber: 667 kHz, 1114 kHz, 1561 kHz, and 2453 kHz with three replications of voltage input maintained at 1000 VAC and flow rate maintained at 16 mL min^{-1} the concentration of the yeast suspension was approximately 60,000 cells mL^{-1} which is in between the "Low" and "Medium" concentrations from the Initial Concentration testing.

The testing procedure was to take a baseline optical signal with the piezoceramic not activated and then activate the piezoceramic for a constant duration and collect the transient signal until stability was achieved. A 60 mL sample was used to collect a baseline voltage, the power amplifier activated for 100 mL with 1000VAC to collect a clear detector voltage, deactivate the power amplifier and collect a 40 mL concentrated portion measured using the Optical Density Detector. The results for the factorial test of the effect of frequency are shown in Table 4.3

Table 4.3 Resonant Frequency testing results with *S. cerevisiae*

	Detector Voltage			Concentration (cfu mL^{-1})				
667kHz	Start	Clear	Conc.	Start	Clear	Conc.	Percent Clarified	Percent Conc.
Rep # 1	1.075	1.118	1.035	60,128	53,954	66,098	10%	10%
Rep # 2	1.080	1.093	1.030	59,398	57,514	66,860	3%	13%
Rep # 3	1.063	1.075	0.977	61,895	60,128	75,177	3%	21%
Average				60,474	57,199	69,378	5%	15%
1114kHz								
Rep # 1	1.093	1.103	1.088	57,514	56,080	58,236	2%	1%
Rep # 2	1.108	1.143	1.000	55,368	50,472	71,514	9%	29%
Rep # 3	1.068	1.143	0.992	61,157	50,472	72,778	17%	19%
Average				58,013	52,341	67,509	13%	24%
1561kHz								
Rep # 1	0.985	1.093	0.885	73,893	57,514	90,747	22%	23%
Rep # 2	1.113	1.160	0.993	54,659	48,148	72,620	12%	33%
Rep # 3	1.058	1.150	0.935	62,638	49,511	82,094	21%	31%
Average				63,730	51,724	81,820	18%	29%
2453kHz								
Rep # 1	1.093	1.128	1.043	57,514	52,552	64,886	9%	13%
Rep # 2	1.065	1.138	0.957	61,600	51,162	78,433	17%	27%
Rep # 3	1.055	1.120	0.915	63,085	53,672	85,499	15%	36%

Average	60,733	52,462	76,272	16%	31%

*grayed cells were thought to be anomalous and were ignored in the averaging.

The percent clarification ranged between 3% and 22%. Likewise, the percent concentration ranged between 10% and 36%. The data were plotted in Figure 4.4 and there appeared to be no slope correlation. An ANOVA was conducted as shown in Table 4.4 and no significant difference was found.

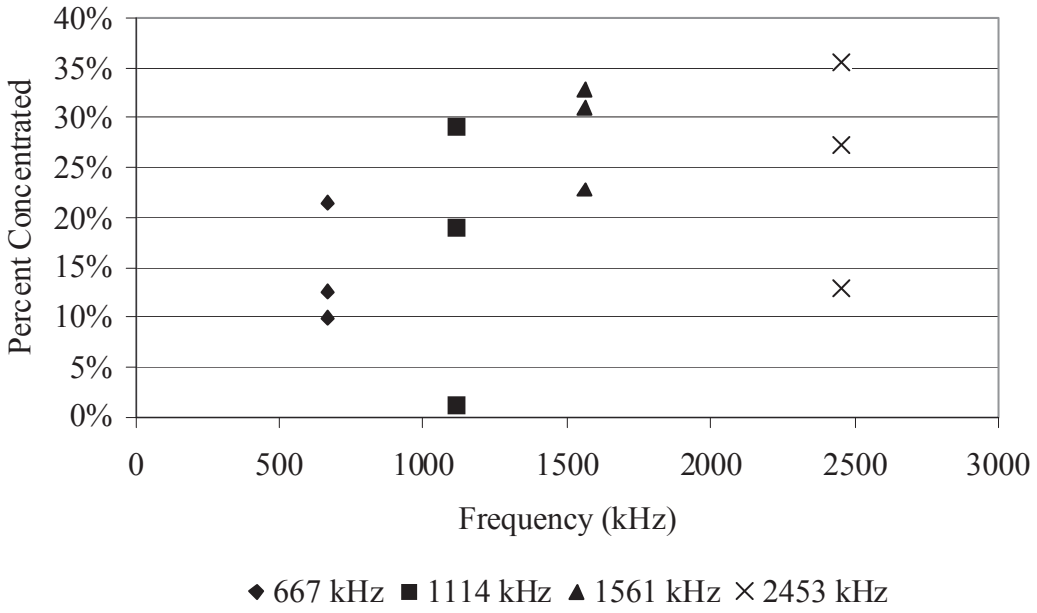

Figure 4.4 Resonant Frequency effect on the concentration of *S. cerevisiae*

Table 4.4 Resonant Frequency effect on the concentration of *S. cerevisiae* ANOVA

Groups	Count	Sum	Average	Variance
667 kHz	3	0.037	0.0123	2E-05
1114 kHz	3	0.0404	0.0135	0.0001
1561 kHz	3	0.0689	0.023	2E-05
2453 kHz	3	0.0604	0.0201	7E-05

ANOVA

Source of Variation	SS	df	MS	F	P-value	F crit
Between Groups	0.0002	3	8E-05	1.339	0.3284	4.0662
Within Groups	0.0005	8	6E-05			
Total	0.0007	11				

4.6 Resonant Frequency Testing with *E. coli*

Three frequencies were tested based on their resonance response with the piezoceramic discs and the chamber: 1561 kHz, 2453, and 2901 kHz with three replications and with the voltage input maintained at 1500 VAC peak-to-peak; the flow rate was maintained at 8 mL min^{-1}. Based on the *S. cerevisiae* results, the lower frequencies were dropped (667 and 1114 kHz) and a higher frequency was added (2901 kHz).

The testing procedure involved recording a baseline optical signal with the piezoceramic not activated, then activate the power amplifier for a constant duration and collect the transient signal until stability was achieved. A 60 mL sample was used to collect a baseline voltage, the power amplifier activated for 100 mL with 1500 VAC to collect a clear detector voltage, deactivate the power amplifier and collect 40 mL more while the concentrated portion was collected in the Optical Density Detector. The results for the factorial test of the effect of frequency are shown in Table 4.5.

Table 4.5 Resonant Frequency testing results with *E. coli*

	Detector Voltage			Concentration (cfu mL^{-1})				
1561 kHz	Start	Clear	Conc.	Start	Clear	Conc.	Percent Clarified	Percent Conc.
Rep # 1	1.267	1.284	1.274	5.79E6	5.34E6	5.60E6	8%	-3%
Rep # 2	1.260	1.240	1.238	5.97E6	6.51E6	6.57E6	-9%	10%
Rep # 3	1.221	1.2058	1.2138	7.06E6	7.48E6	7.26E6	-6%	3%
Average				6.27E6	6.44E6	6.48E6	-2%	3%
2453 kHz								
Rep # 1	1.280	1.280	1.264	5.43E6	5.44E6	5.87E6	0%	8%
Rep # 2	1.212	1.205	1.207	7.32E6	7.51E6	7.45E6	-3%	2%
Rep # 3	1.216	1.204	1.222	7.19E6	7.54E6	7.03E6	-5%	-2%
Average				6.64E6	6.83E6	6.78E6	-4%	0%
2901 kHz								
Rep # 1	1.284	1.335	1.276	5.33E6	3.99E6	5.55E6	25%	4%
Rep # 2	1.260	1.242	1.249	5.99E6	6.47E6	6.28E6	-8%	5%
Rep # 3	1.216	1.228	1.204	7.19E6	6.86E6	7.53E6	5%	5%
Average				6.17E6	5.77E6	6.45E6	7%	5%

The percent clarification ranged between -9% and 25%. Likewise, the percent concentration ranged between -3% and 10%. The data were plotted in Figure 4.5 and there appeared to be no slope correlation. An ANOVA was conducted as shown in Table 4.6 and no significant difference was found. However, the frequency at 2901 kHz seemed to give the most consistent results; as such, this frequency was used for all the following testing procedures.

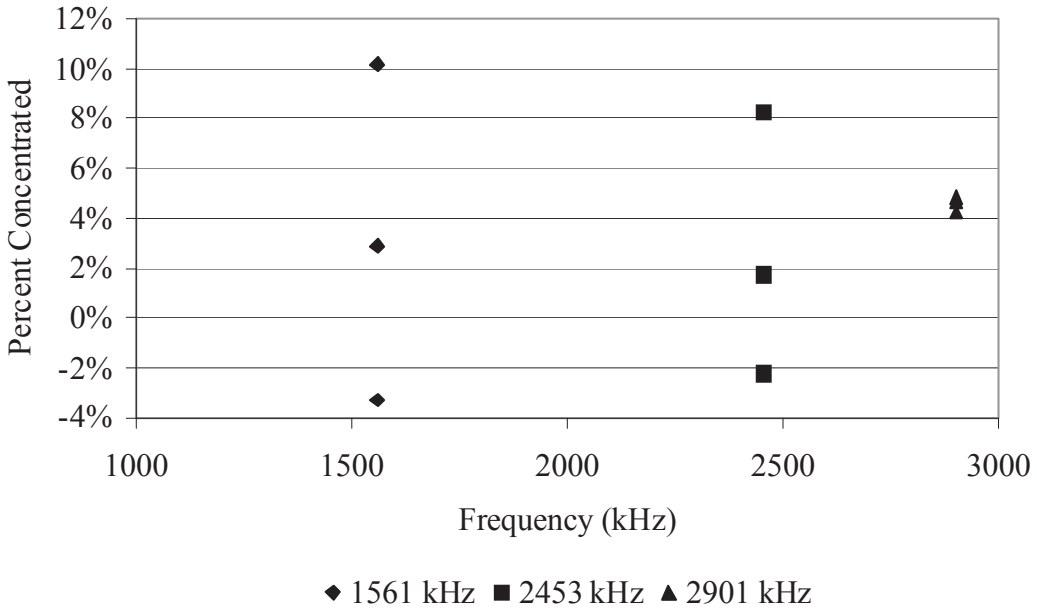

Figure 4.5 Resonant Frequency effect on the concentration of *E. coli*

Table 4.6 Resonant Frequency effect on the concentration of *E. coli* ANOVA

Groups	Count	Sum	Average	Variance
1561 kHz	3	0.0058	0.0019	2E-05
2453 kHz	3	0.0048	0.0016	1E-05
2901 kHz	3	0.0086	0.0029	3E-08

ANOVA

Source of Variation	SS	df	MS	F	P-value	F crit
Between Groups	2E-06	2	1E-06	0.1318	0.879	5.1433
Within Groups	6E-05	6	9E-06			
Total	6E-05	8				

4.7 Flow Rate Testing with *S. cerevisiae*

Three flow rates were tested based on previous testing on mouse hybridoma cells as reported by Wang et al. (2004). The flow rates were 8, 16, and 32 mL min^{-1}. Three replications of each condition were tested.

The testing was completed with the following testing conditions: the frequency was maintained around 1560 kHz and adjusted to maintain resonance; the voltage input was maintained at 1000 VAC peak-to-peak; the flow rates were maintained at either 8, 16, or 32 mL min^{-1}.

The testing procedure was to take a baseline sample of 60 mL to collect a starting voltage, activate the power amplifier for 100 mL with 1000 VAC to collect a clear detector voltage, deactivate the power amplifier and collect 40 mL more while the concentrated portion was collected in the Optical Density Detector. The results for the factorial test of the effect of flow rate are shown in Table 4.7.

Table 4.7 Flow Rate testing results with *S. cerevisiae*

	Detector Voltage			Concentration (cfu mL^{-1})				
8 mL min^{-1}	Start	Clear	Conc.	Start	Clear	Conc.	Percent Clarified	Percent Conc.
Rep # 1	1.050	1.145	0.878	63,833	50,197	91,997	21%	44%
Rep # 2	1.075	1.180	0.907	60,128	45,457	86,881	24%	44%
Rep # 3	1.069	1.177	0.884	61,009	45,857	90,925	25%	49%
Average				61,657	47,170	89,934	24%	46%
16 mL min^{-1}								
Rep # 1	1.029	1.082	0.920	67,013	59,106	84,641	12%	26%
Rep # 2	1.029	1.080	0.900	67,013	59,398	88,101	11%	31%
Rep # 3	0.984	1.056	0.871	74,053	62,936	93,257	15%	26%
Average				69,360	60,480	88,666	13%	28%
32 mL min^{-1}								
Rep # 1	0.980	1.012	0.934	74,694	69,636	82,263	7%	10%
Rep # 2	0.990	1.019	0.938	73,096	68,551	81,590	6%	12%
Rep # 3	0.991	1.015	0.940	72,937	69,170	81,255	5%	11%
Average				73,576	69,119	81,703	6%	11%

The percent clarification ranged between 5% and 25%. Likewise, the percent concentration ranged between 10% and 49%. The data were plotted in Figure 4.6 and there appeared to be a negative slope correlation. An ANOVA was conducted as shown in Table 4.8 and a significant difference was found.

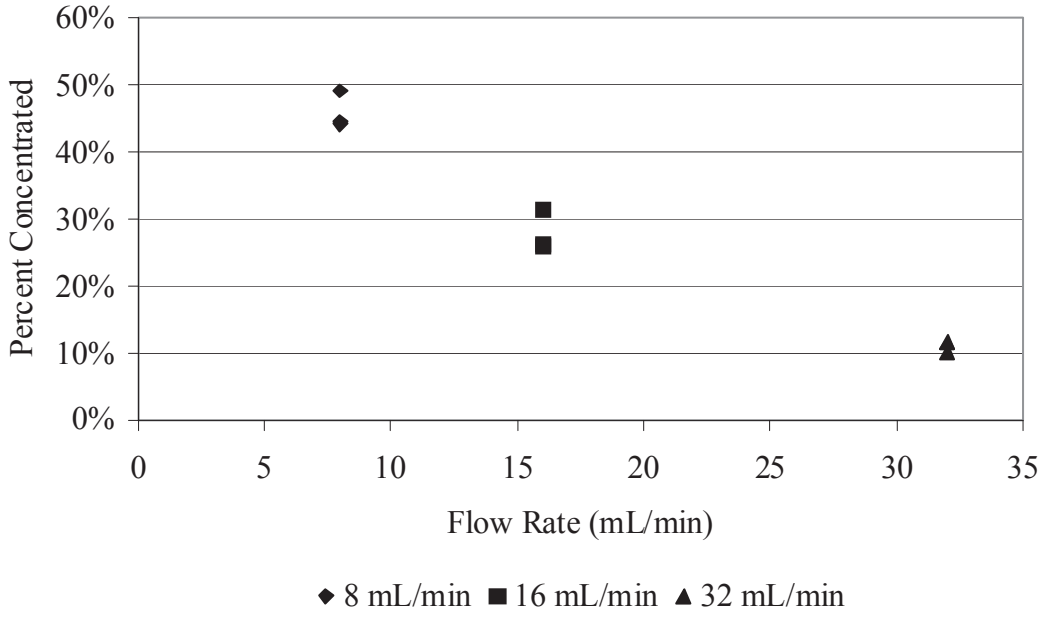

Figure 4.6 Flow Rate effect on the concentration of *S. cerevisiae*

Table 4.8 Flow Rate effect on the concentration of *S. cerevisiae* ANOVA

Groups	Count	Sum	Average	Variance
8 mL min^{-1}	3	0.1027	0.0342	3E-06
16 mL min^{-1}	3	0.0662	0.0221	5E-06
32 mL min^{-1}	3	0.0281	0.0094	4E-07

ANOVA

Source of Variation	SS	df	MS	F	P-value	F crit
Between Groups	0.0009	2	0.0005	166.62	6E-06	5.1433
Within Groups	2E-05	6	3E-06			
Total	0.0009	8				

4.8 Flow Rate Testing with *E. coli*

Three flow rates were tested based on previous testing on the yeast. The flow rates were 4, 8, and 16 mL min^{-1}. Three replications of each condition were tested.

The testing was completed with the following testing conditions: the frequency was maintained around 1560 kHz and adjusted to maintain resonance; the voltage input was maintained at 1500 VAC peak-to-peak; the flow rates were maintained at 4, 8, or 16 mL min^{-1}.

The testing procedure was to take a baseline sample of 60 mL to collect a starting voltage, activate the power amplifier for 100 mL with 1500 VAC to collect a clear detector voltage, deactivate the power amplifier and collect 40 mL more while the concentrated portion was collected in the Optical Density Detector. The results for the factorial test of the effect of flow rate are shown in Table 4.9.

Table 4.9 Flow Rate testing results with *E. coli*

	Detector Voltage			Concentration (cfu mL^{-1})				
4 mL min^{-1}	Start	Clear	Conc.	Start	Clear	Conc.	Percent Clarified	Percent Conc.
Rep # 1	1.066	1.059	1.063	1.17E7	1.19E7	1.18E7	-2%	1%
Rep # 2	1.111	1.069	1.109	1.03E7	1.16E7	1.04E7	-13%	1%
Rep # 3	1.121	1.108	1.119	1.00E7	1.04E7	1.01E7	-4%	1%
Average				1.07E7	1.13E7	1.07E7	-6%	1%
8 mL min^{-1}								
Rep # 1	1.072	1.053	1.057	1.15E7	1.21E7	1.20E7	-5%	4%
Rep # 2	1.111	1.108	1.102	1.03E7	1.04E7	1.06E7	-1%	3%
Rep # 3	1.095	1.086	1.094	1.08E7	1.11E7	1.08E7	-3%	0%
Average				1.09E7	1.12E7	1.11E7	-3%	2%
16 mL min^{-1}								
Rep # 1	1.041	1.064	1.059	1.25E7	1.18E7	1.19E7	6%	-5%
Rep # 2	1.087	1.086	1.089	1.10E7	1.11E7	1.10E7	0%	0%
Rep # 3	1.126	1.113	1.124	9.84E6	1.02E7	9.90E6	-4%	1%
Average				1.11E7	1.10E7	1.09E7	1%	-2%

The percent clarification ranged between -13% and 6%. Likewise, the percent concentration ranged between -5% and 4%. The data were plotted in Figure 4.7 and there

appeared to be no slope correlation. An ANOVA was conducted as shown in Table 4.10 and no significant difference was found.

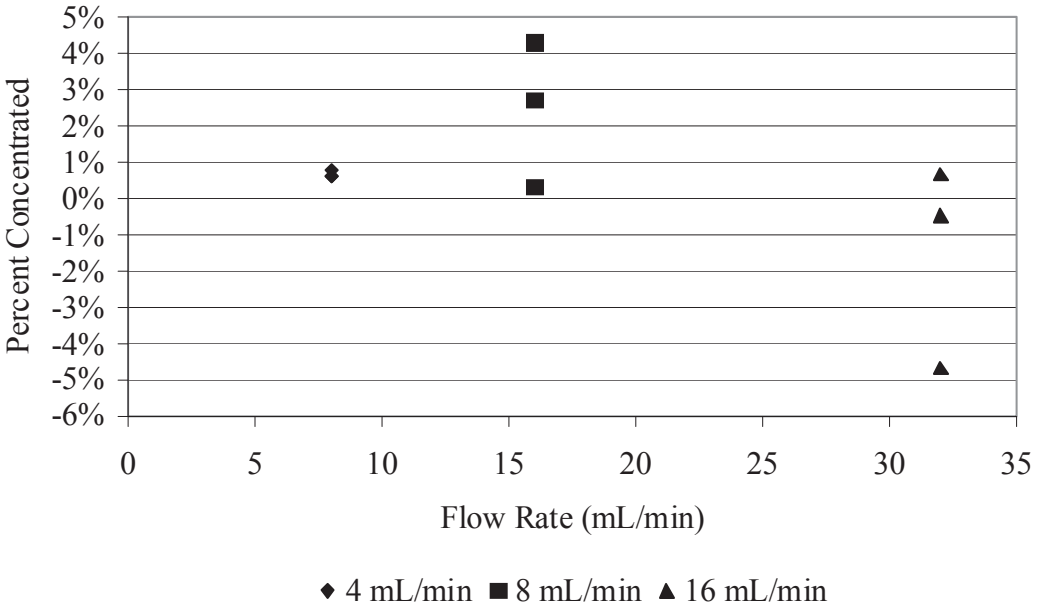

Figure 4.7 Flow Rate effect on the concentration of *E. coli*

Table 4.10 Flow Rate effect on the concentration of *E. coli* ANOVA

Groups	Count	Sum	Average	Variance
4 mL min^{-1}	3	0.0012	0.0004	3E-09
8 mL min^{-1}	3	0.0045	0.0015	1E-06
16 mL min^{-1}	3	-0.003	-9E-04	3E-06

ANOVA

Source of Variation	SS	df	MS	F	P-value	F crit
Between Groups	9E-06	2	4E-06	2.9206	0.1301	5.1433
Within Groups	9E-06	6	2E-06			
Total	2E-05	8				

4.9 Voltage Input Testing with *S. cerevisiae*

Three voltage levels were tested based on allowable limits of the power amplifier and excessive heat generation in the chamber. The voltage levels were 1000, 1500, and 2000 peak-to-peak volts AC (VAC). There were three replications of each test.

The testing was completed with the following testing conditions: the frequency was maintained around 1560 kHz and adjusted to maintain resonance; the voltage input

was maintained at 1000, 1500, or 2000 VAC peak-to-peak; the flow rate was maintained at 16 mL min^{-1}.

The testing procedure was to take a baseline sample of 60 mL to collect a starting voltage, activate the power amplifier for 100 mL with 1000, 1500, or 2000 VAC to collect a clear detector voltage, deactivate the power amplifier and collect 40 mL more while the concentrated portion was collected in the Optical Density Detector. The results for the factorial test of the effect of voltage are shown in Table 4.11.

Table 4.11 Voltage Input testing results with *S. cerevisiae*

	Detector Voltage			Concentration (cfu mL^{-1})				
1000 VAC	Start	Clear	Conc.	Start	Clear	Conc.	Percent Clarified	Percent Conc.
Rep # 1	1.020	1.074	0.907	68,396	60,275	86,881	12%	27%
Rep # 2	1.006	1.069	0.911	70,572	61,009	86,188	14%	22%
Rep # 3	1.001	1.037	0.901	71,356	65,794	87,926	8%	23%
Average				70,108	62,359	86,998	11%	24%
1500 VAC								
Rep # 1	1.015	1.120	0.745	69,170	53,672	117,857	22%	70%
Rep # 2	0.996	1.118	0.744	72,145	53,954	118,068	25%	64%
Rep # 3	0.983	1.100	0.740	74,213	56,509	118,917	24%	60%
Average				71,843	54,712	118,281	24%	65%
2000 VAC								
Rep # 1	1.015	1.218	0.700	69,170	40,467	127,665	41%	85%
Rep # 2	1.015	1.209	0.601	69,170	41,634	151,671	40%	119%
Rep # 3	0.996	1.212	0.613	72,145	41,244	148,559	43%	106%
Average				70,161	41,115	142,632	41%	103%

The percent clarification ranged between 8% and 43%. Likewise, the percent concentration ranged between 22% and 119%. These represent the largest percents concentrated as seen in the one-way factorial testing. The data were plotted in Figure 4.8 and there appears to be a positive slope correlation. An ANOVA was conducted as shown in Table 4.12 and a significant difference was found (p=0.0001).

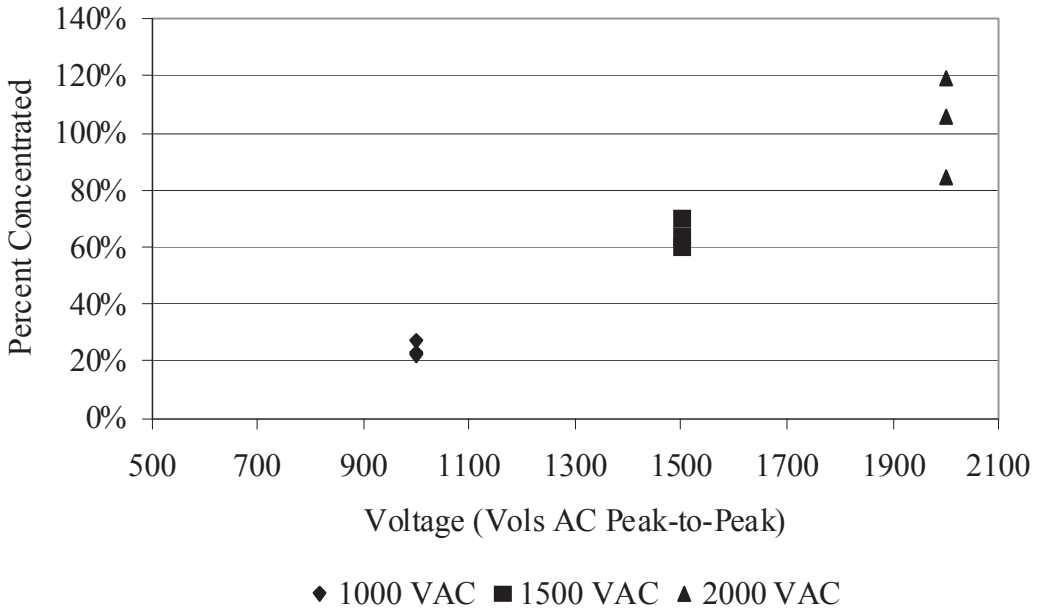

Figure 4.8 Voltage Input effect on the concentration of *S. cerevisiae*

Table 4.12 Voltage Input effect on the concentration of *S. cerevisiae* ANOVA

Groups	Count	Sum	Average	Variance
1000 VAC	3	0.0581	0.0194	4E-06
1500 VAC	3	0.1339	0.0446	9E-06
2000 VAC	3	0.19	0.0633	6E-05

ANOVA

Source of Variation	SS	df	MS	F	P-value	F crit
Between Groups	0.0029	2	0.0015	60.009	0.0001	5.1433
Within Groups	0.0001	6	2E-05			
Total	0.0031	8				

4.10 Voltage Input Testing with *E. coli*.

Similarly to the yeast testing procedure the three voltage levels were tested based on allowable limits of the power amplifier and excessive heat generation in the chamber. The voltage levels were 1000, 1500, and 2000 peak-to-peak volts AC. Each test was replicated three times.

The testing was completed with the following testing conditions: the frequency was maintained around 2900 kHz and adjusted to maintain resonance; the voltage input

was maintained at 1000, 1500, or 2000 VAC peak-to-peak; the flow rate was maintained at 8 mL min^{-1}.

The testing procedure was to take a baseline sample of 60 mL to collect a starting voltage, activate the power amplifier for 100 mL with 1000, 1500, or 2000 VAC to collect a clear detector voltage, deactivate the power amplifier and collect 40 mL more while the concentrated portion was collected in the Optical Density Detector. The results for the one way factorial test of the effect of voltage are shown in Table 4.13.

Table 4.13 Voltage Input testing results with *E. coli*.

	Detector Voltage			Concentration (cfu mL^{-1})				
1000 VAC	Start	Clear	Conc.	Start	Clear	Conc.	Percent Clarified	Percent Conc.
Rep # 1	1.288	1.285	1.281	5.24E6	5.29E6	5.41E6	-1%	3%
Rep # 2	1.277	1.280	1.278	5.51E6	5.44E6	5.49E6	1%	0%
Rep # 3	1.275	1.280	1.272	5.57E6	5.43E6	5.65E6	3%	1%
Average				5.44E6	5.39E6	5.52E6	1%	1%
1500 VAC								
Rep # 1	1.280	1.276	1.289	5.44E6	5.54E6	5.21E6	-2%	-4%
Rep # 2	1.308	1.304	1.295	4.70E6	4.80E6	5.04E6	-2%	7%
Rep # 3	1.297	1.293	1.285	5.00E6	5.09E6	5.30E6	-2%	6%
Average				5.04E6	5.15E6	5.18E6	-2%	3%
2000 VAC								
Rep # 1	1.290	1.287	1.290	5.16E6	5.24E6	5.18E6	-2%	0%
Rep # 2	1.275	1.281	1.295	5.56E6	5.42E6	5.05E6	3%	-9%
Rep # 3	1.297	1.295	1.292	4.99E6	5.04E6	5.12E6	-1%	3%
Average				5.24E6	5.23E6	5.12E6	0%	-2%

The percent clarification ranged between -2% and 3%. Likewise, the percent concentration ranged between -9% and 7%. The data were plotted in Figure 4.9 and there did not appear to be any slope correlation. An ANOVA was conducted as shown in Table 4.14 and no significant difference was found.

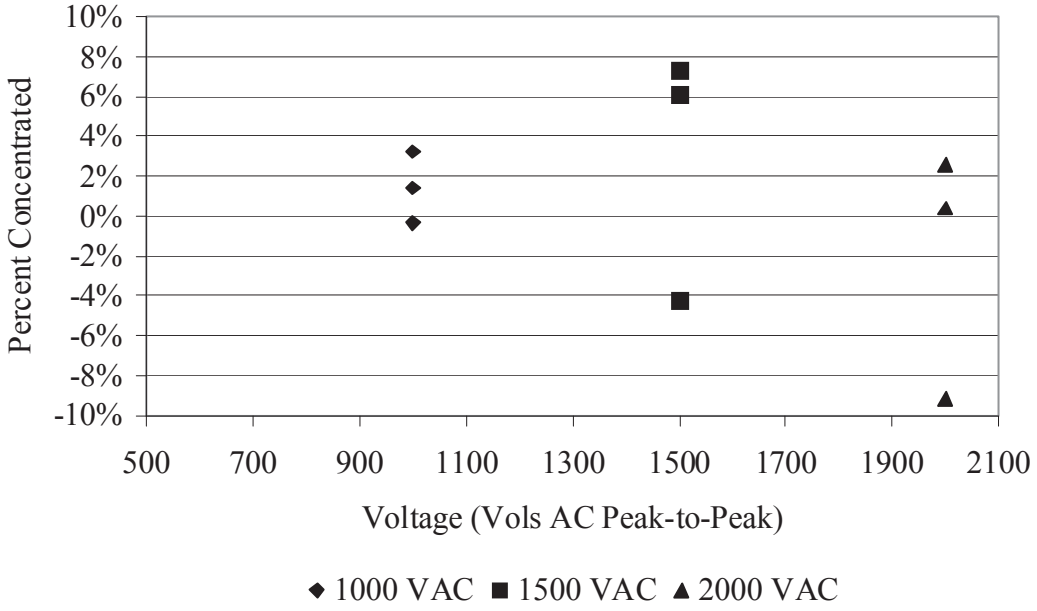

Figure 4.9 Voltage Input effect on the concentration of *E. coli*

Table 4.14 Voltage Input effect on the concentration of *E. coli* ANOVA

Groups	Count	Sum	Average	Variance
1000 VAC	3	0.0027	0.0009	1E-06
1500 VAC	3	0.0056	0.0019	2E-05
2000 VAC	3	-0.004	-0.001	2E-05

ANOVA

Source of Variation	SS	df	MS	F	P-value	F crit
Between Groups	2E-05	2	9E-06	0.7469	0.5133	5.1433
Within Groups	7E-05	6	1E-05			
Total	9E-05	8				

4.11 Volume Throughput Testing with *S. cerevisiae*

Three levels of volume throughput were tested based on allowable limits of the syringe pumps. The volumes with the voltage applied were 50, 100, and 200 mL. Three replications of samples were tested.

The testing was completed with the following testing conditions: the frequency was maintained around 1560 kHz and adjusted to maintain resonance; the voltage input was maintained at 1000 VAC peak-to-peak; the flow rate was maintained at 16 mL min^{-1}.

The testing procedure was to take a baseline sample of 60 mL to collect a starting voltage, activate the power amplifier for 50, 100, or 200 mL with 1000 VAC to collect a clear detector voltage, deactivate the power amplifier and collect 40 mL more while the concentrated portion was collected in the Optical Density Detector. The results for the factorial test of the effect of volume throughput are shown in Table 4.15.

Table 4.15 Volume Throughput testing results with *S. cerevisiae*

	Detector Voltage			Concentration (cfu mL^{-1})				
50 mL	Start	Clear	Conc.	Start	Clear	Conc.	Percent Clarified	Percent Conc.
Rep # 1	1.041	1.091	0.960	65,188	57,802	77,940	11%	20%
Rep # 2	1.035	1.090	0.967	66,098	57,947	76,797	12%	16%
Rep # 3	1.015	1.072	0.949	69,170	60,568	79,755	12%	15%
Average				66,819	58,772	78,164	12%	17%
100 mL								
Rep # 1	1.037	1.086	0.917	65,794	58,526	85,155	11%	29%
Rep # 2	1.018	1.080	0.903	68,705	59,398	87,577	14%	27%
Rep # 3	1.012	1.075	0.865	69,636	60,128	94,345	14%	35%
Average				68,045	59,350	89,026	13%	31%
200 mL								
Rep # 1	1.028	1.091	0.906	67,166	57,802	87,055	14%	30%
Rep # 2	1.025	1.083	0.825	67,626	58,961	101,799	13%	51%
Rep # 3	1.023	1.083	0.780	67,934	58,961	110,629	13%	63%
Average				67,575	58,575	99,828	13%	48%

The percent clarification ranged between 11% and 14%. Likewise, the percent concentration ranged between 15% and 63%. The data were plotted in Figure 4.10 and there appeared to be a positive slope correlation. An ANOVA was conducted as shown in Table 4.16 and a significant difference was found ($p=0.0207$).

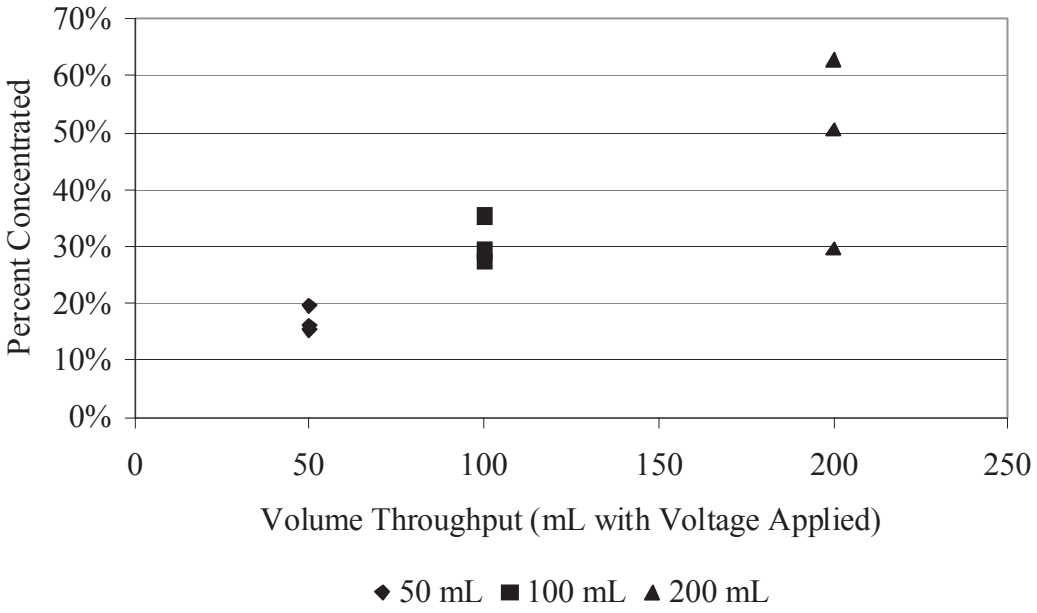

Figure 4.10 Volume Throughput effect on the concentration of *S. cerevisiae*

Table 4.16 Volume Throughput effect on the concentration of *S. cereisiae* ANOVA

Groups	Count	Sum	Average	Variance
50 mL	3	0.0424	0.0141	3E-06
100 mL	3	0.0723	0.0241	8E-06
200 mL	3	0.1039	0.0346	0.0001

ANOVA

Source of Variation	SS	df	MS	F	P-value	F crit
Between Groups	0.0006	2	0.0003	7.9273	0.0207	5.1433
Within Groups	0.0002	6	4E-05			
Total	0.0009	8				

4.12 Volume Throughput Testing with *E. coli*

Based off the yeast testing procedure, the 50 mL volume throughput with the power amplifier actuated did not perform well; only the 100 and 200mL levels were chosen for testing. A 300mL testing level was desired, however, a pulsation would have been introduced while switching syringes on the pumps being used. Therefore, two levels of volume throughput were tested based on allowable limits of the syringe pumps. The volumes with the voltage applied were 100 and 200 mL. Three replications of samples were tested.

The testing was completed with the following testing conditions: the frequency was maintained around 2900 kHz and adjusted to maintain resonance; the voltage input was maintained at 1500 VAC peak-to-peak; the flow rate was maintained at 8 mL min^{-1}.

The testing procedure was to take a baseline sample of 60 mL to collect a starting voltage, activate the power amplifier for 50, 100, or 200 mL with 1000 VAC to collect a clear detector voltage, deactivate the power amplifier and collect 40 mL more while the concentrated portion was collected in the Optical Density Detector. The results for the factorial test of the effect of volume throughput are shown in Table 4.17.

Table 4.17 Volume Throughout testing results with *E. coli*.

	Detector Voltage			Concentration (cells mL^{-1})				
100 mL	Start	Clear	Conc.	Start	Clear	Conc.	Percent Clarified	Percent Conc.
Rep # 1	1.278	1.263	1.269	5.50E6	5.90E6	5.73E6	-7%	4%
Rep # 2	1.212	1.191	1.190	7.30E6	7.91E6	7.94E6	-8%	9%
Rep # 3	1.194	1.182	1.180	7.82E6	8.18E6	8.23E6	-5%	5%
Average				6.87E6	7.33E6	7.30E6	-7%	6%
200 mL								
Rep # 1	1.257	1.272	1.277	6.05E6	5.65E6	5.51E6	7%	-9%
Rep # 2	1.217	1.222	1.213	7.17E6	7.01E6	7.27E6	2%	1%
Rep # 3	1.198	1.183	1.198	7.72E6	8.14E6	7.72E6	-5%	0%
Average				6.98E6	6.93E6	6.83E6	1%	-3%

The percent clarification ranged between -8% and 7%. Likewise, the percent concentration ranged between -9% and 9%. The data were plotted in Figure 4.11 and there appeared to be a positive slope correlation. An ANOVA was conducted as shown in Table 4.18 and no significant difference was found.

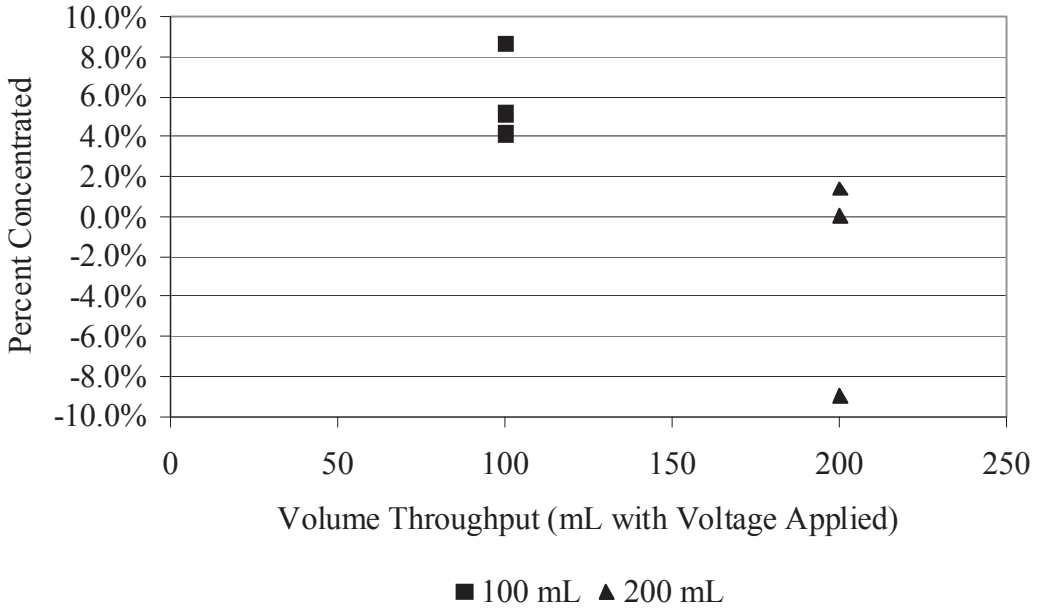

Figure 4.11 Volume Throughput effect on the concentration of *E. coli*

Table 4.18 Volume Throughput effect on the concentration of *E. coli* ANOVA

Groups	Count	Sum	Average	Variance
100 mL	3	0.0111	0.0037	2E-06
200 mL	3	-0.005	-0.002	1E-05

ANOVA

Source of Variation	SS	df	MS	F	P-value	F crit
Between Groups	4E-05	1	4E-05	5.4454	0.0799	7.7086
Within Groups	3E-05	4	8E-06			
Total	8E-05	5				

4.13 Foam Density Testing with *S. cerevisiae*

Three different reticulated polyurethane foams were tested based on research conducted by Wang Z. et al. (2004). The foam densities chosen were 45, 60, and 100 pores per inch (PPI). Three replications of samples were tested.

The testing was completed with the following testing conditions: the frequency was maintained around 1560 kHz and adjusted to maintain resonance; the voltage input was maintained at 1000 VAC peak-to-peak; the flow rate was maintained at 16 mL min^{-1}.

The testing procedure was to take a baseline sample of 60 mL to collect a starting voltage, activate the power amplifier for 100 mL with 1000 VAC to collect a clear detector voltage, deactivate the power amplifier and collect 40 mL more while the concentrated portion was collected in the Optical Density Detector. The results for the factorial test of the effect of foam density are shown in Table 4.19.

Table 4.19 Foam Density testing results with *S. cerevisiae*

	Detector Voltage			Concentration (cfu mL^{-1})				
45 PPI	Start	Clear	Conc.	Start	Clear	Conc.	Percent Clarified	Percent Conc.
Rep # 1	1.028	1.078	0.922	67,166	59,690	84,299	11%	26%
Rep # 2	1.008	1.080	0.948	70,259	59,398	79,921	15%	14%
Rep # 3	1.000	1.064	0.916	71,514	61,747	85,327	14%	19%
Average				69,646	60,278	83,182	13%	20%
60 PPI								
Rep # 1	1.018	1.057	0.955	68,705	62,787	78,762	9%	15%
Rep # 2	0.916	0.952	0.832	85,327	79,258	100,469	7%	18%
Rep # 3	0.976	1.008	0.872	75,338	70,259	93,076	7%	24%
Average				76,457	70,768	90,769	7%	19%
100 PPI								
Rep # 1	1.009	1.072	0.907	70,103	60,568	86,881	14%	24%
Rep # 2	0.955	1.015	0.880	78,762	69,170	91,639	12%	16%
Rep # 3	0.984	1.036	0.872	74,053	65,946	93,076	11%	26%
Average				74,306	65,228	90,532	12%	22%

The percent clarification ranged between 7% and 15%. Likewise, the percent concentration ranged between 14% and 26%. The data were plotted in Figure 4.12 and there appeared to be no slope correlation. An ANOVA was conducted as shown in Table 4.20 and there was no significant difference found.

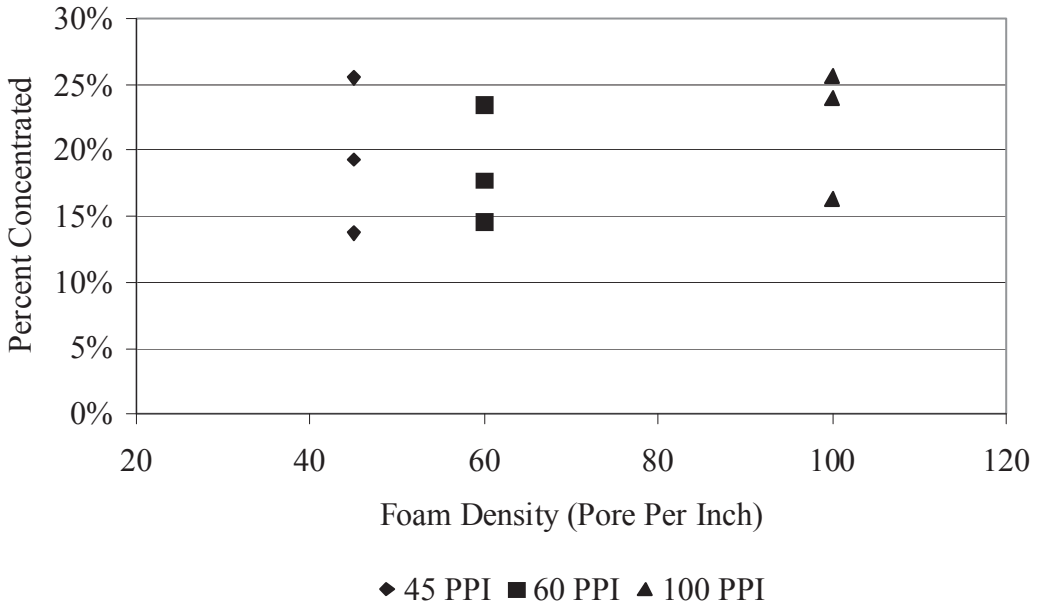

Figure 4.12 Foam Density effect on the concentration of *S. cerevisiae*

Table 4.20 Foam Density effect on the concentration of *S. cerevisiae* ANOVA

Groups	Count	Sum	Average	Variance
45 PPI	3	0.0478	0.0159	2E-05
60 PPI	3	0.0455	0.0152	1E-05
100 PPI	3	0.0531	0.0177	1E-05

ANOVA

Source of Variation	SS	df	MS	F	P-value	F crit
Between Groups	1E-05	2	0.0026	0.3421	0.7232	5.143
Within Groups	9E-05	6	0.0078			
Total	1E-04	8				

4.14 Foam Density Testing with *E. coli*

Similar to the yeast testing procedure, three different reticulated polyurethane foams were tested. Although there were no statistical differences found with the different foam porosities with the yeast, it was believed there would be a difference with the smaller *E. coli*. The foam densities used were 45, 60, and 100 pores per inch (PPI). Three replications of samples were tested.

The testing was completed with the following testing conditions: the frequency was maintained around 2900 kHz and adjusted to maintain resonance; the voltage input was maintained at 1500 VAC peak-to-peak; the flow rate was maintained at 8 mL min^{-1}.

The testing procedure was to take a baseline sample of 60 mL to collect a starting voltage, activate the power amplifier for 100 mL with 1500 VAC to collect a clear detector voltage, deactivate the power amplifier and collect 40 mL more while the concentrated portion was collected in the Optical Density Detector. The results for the factorial test of the effect of foam density are shown in Table 4.21.

Table 4.21 Foam Density testing results with *E. coli*.

	Detector Voltage			Concentration (cfu mL^{-1})				
45 PPI	Start	Clear	Conc.	Start	Clear	Conc.	Percent Clarified	Percent Conc.
Rep # 1	1.352	1.364	1.353	3.57E6	3.27E6	3.53E6	8%	-1%
Rep # 2	1.255	1.285	1.234	6.11E6	5.30E6	6.69E6	13%	9%
Rep # 3	1.189	1.182	1.166	7.97E6	8.16E6	8.64E6	-2%	8%
Average				5.88E6	5.57E6	6.28E6	6%	6%
60 PPI								
Rep # 1	1.129	1.157	1.150	9.74E6	8.90E6	9.12E6	9%	-6%
Rep # 2	1.168	1.178	1.183	8.57E6	8.28E6	8.13E6	3%	-5%
Rep # 3	1.252	1.251	1.244	6.20E6	6.23E6	6.42E6	0%	4%
Average				8.17E6	7.80E6	7.89E6	4%	-3%
100 PPI								
Rep # 1	1.333	1.344	1.337	4.05E6	3.76E6	3.95E6	7%	-2%
Rep # 2	1.294	1.289	1.278	5.06E6	5.19E6	5.48E6	-3%	8%
Rep # 3	1.277	1.276	1.262	5.52E6	5.55E6	5.92E6	0%	7%
Average				4.88E6	4.83E6	5.12E6	1%	4%

The percent clarification ranged between -2% and 13%. Likewise, the percent concentration ranged between -6% and 9%. These represent a negligible difference. The data was plotted in Figure 4.13 and there appears to be no slope correlation. An ANOVA was conducted as shown in Table 4.22 and there was no significant difference ($P>0.05$).

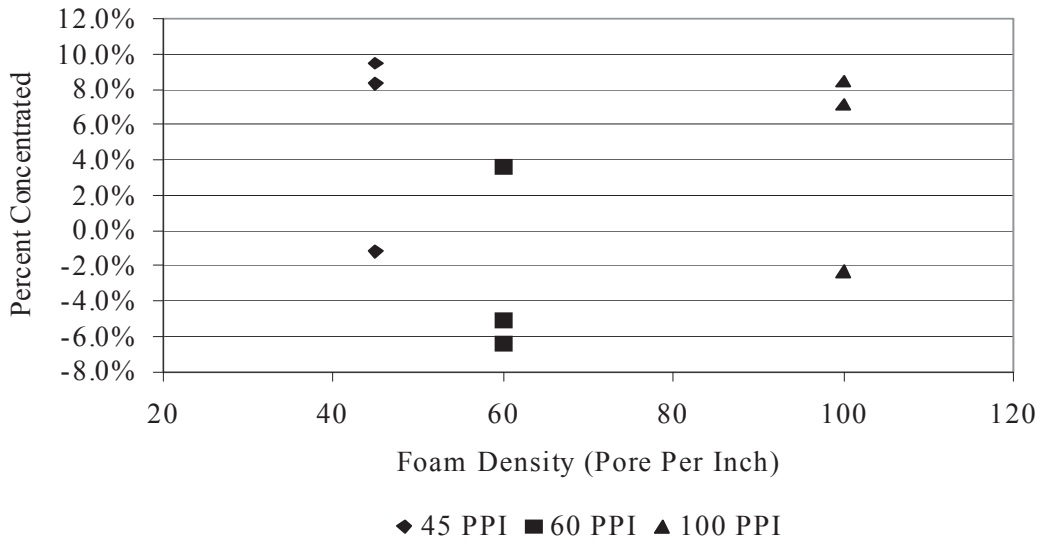

Figure 4.13 Foam Density effect on the concentration of *E. coli*

Table 4.22 Foam Density effect on the concentration of *E. coli* ANOVA

Groups	Count	Sum	Average	Variance
45 PPI	3	0.01	0.0033	1E-05
60 PPI	3	-0.005	-0.002	1E-05
100 PPI	3	0.0081	0.0027	1E-05

ANOVA

Source of Variation	SS	df	MS	F	P-value	F crit
Between Groups	4E-05	2	2E-05	1.7332	0.2546	5.1433
Within Groups	8E-05	6	1E-05			
Total	0.0001	8				

4.15 Ideal Conditions Testing with *S. cerevisiae*

Based on the results of the above testing an optimum testing condition was chosen. Conditions for ultrasonic concentration selected were: 45 PPI Foam, 2000 VAC, 200 mL with voltage on, 1560 kHz, and 8 mL min^{-1}. Samples were tested at the ideal conditions with four replications.

The testing protocol was as follows: the frequency was maintained around 1560 kHz and adjusted to maintain resonance; the voltage input was maintained at 2000 VAC peak-to-peak; the flow rate was maintained at 8 mL min^{-1}.

The testing procedure was to take a baseline sample of 60 mL to collect a starting voltage, activate the power amplifier for 200 mL with 2000 VAC to collect a clear detector voltage, deactivate the power amplifier and collect 40 mL more while the concentrated portion was collected in the Optical Density Detector. The results for the ideal testing conditions are shown in Table 4.23.

Table 4.23 Ideal Conditions testing results of *S. cerevisiae*

	Detector Voltage			Concentration (cells mL^{-1})				
	Start	Clear	Conc.	Start	Clear	Conc.	Percent Clarified	Percent Conc.
Rep # 1	1.031	1.193	0.792	66,708	43,732	108,226	34%	62%
Rep # 2	0.990	1.171	0.546	73,096	46,662	166,781	36%	128%
Rep # 3	0.973	1.127	0.476	75,823	52,691	188,380	31%	148%
Rep # 4	0.945	1.085	0.350	80,420	58,671	236,788	27%	194%
Average				76,446	52,675	197,316	32%	133%

It was noticed the percent clarified ranged from 27% to 36% while the percent concentrated ranged from 62% to 194%. A relatively large variation in percent concentrated values was also noticed. This variation was considered to result from the accumulation of yeast in the chamber as the tests progressed.

4.16 Ideal Conditions Testing with *E. coli*

After the initial testing procedures, no statistical differences were found using the different treatments and levels of voltage, frequency, flow rate, foam density, or volume throughout. As such, no ideal conditions testing was performed. However, some additional testing was done; similar to the ideal conditions of the yeast testing the slowest flow rate (4 mL min^{-1}) with the 45ppi reticulated foam, 2000 VAC, at 1560 kHz was tested with no significant difference was measured.

4.17 Transient standing wave with *E. coli* testing

A brief concentration response was noticed during the testing, where after the power amplifier was turned on, an increase in the voltage above the baseline condition was noticed – inferring a decrease in cells going though the Optical Density Detector. However, after 2 minutes (see point C on Figure 4.14), the voltage decreased below the baseline condition –inferring an increase in cell concentration passing through the Optical

Density Detector. This would have been acceptable, but the cell concentration was hypothesized to have been concentrated in the chamber under a steady standing wave and then the temperature increase changed the speed of sound properties in the liquid medium which henceforth stopped the concentration forces and the cells exited the chamber and the cell concentration increased in the Optical Density Detector even though the power amplifier was still sending the –supposedly—correct frequency to the sound-source piezoceramic. This short concentration effect is shown in Figure 4.14.

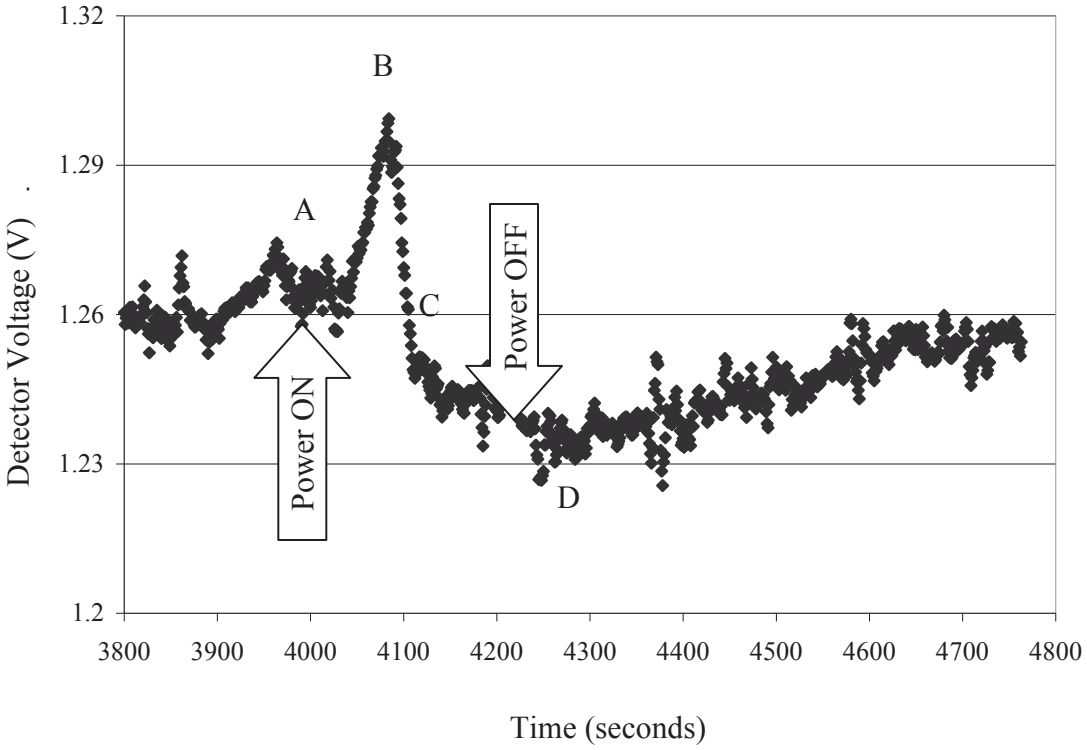

Figure 4.14 Plot sensor voltage data collection with a short concentration cycle.

As seen in Figure 4.14, "A" was when the baseline voltage had been collected and the power amplifier was turned on. "B" shows an increase in the detector voltage, or a decrease in cell concentration through the Optical Density Detector which infers cells being concentrated in the Ultrasonic chamber. "C" shows a premature drop in detector voltage signifying an increase in cells passing through the Optical Density Detector. "D" shows a voltage below the baseline voltage which signifies that cells in the ultrasonic chamber exited without any ultrasonic forces holding them from the drag forces pulling them away.

CHAPTER 5 : DISCUSSION

The Ultrasonic Concentration prototype was found to be successful for concentrating yeast up to 200%; however the concentration effect with *E. coli* was unexpectedly negligible. It was determined from an ANOVA that Flow Rate, Voltage Input, and Volume Throughput had a significant effect on concentrating yeast. No statistically significant variables were found for *E. coli* concentration.

Flow rate is significant because of Stokes drag force equation previously seen in Equation 1.3 $\left(F_{Drag} = -6\pi\mu Rv\right)$. Equation 1.3 shows that the drag force is linearly related to the fluid viscosity, particle radius, and the fluid velocity. Changes in fluid velocity has a significant effect on the grad force and therefore the number of microparticles able to be held in the acoustic resonance chamber.

Voltage input is significant because the increased movement of the piezoceramic increased the *Acoustic Power* in the chamber which increased the *Acoustic Energy Density* or E_{ac} described in Equation 1.4. $F_{AC} = 4\pi R^3 k E_{ac} \Phi(\beta, \rho)$

Furthermore, the voltage input to the piezoceramic and the mechanical displacement of the piezoceramic are linearly proportional, it was also expected that the concentration efficiency should be linearly proportional to the voltage input and the ultrasonic radiation force.

The cell size was very important in the ability to concentrate *S. cerevisiae* versus *E. coli*. Previously shown in Figure 1.11, there is a large size discrepancy between the yeast and bacteria. Going back to the Ultrasonic Radiation Force (F_{ac}) being proportional to the volume ($4/3\pi R^3$, for a sphere). It is important to mention the large volumetric difference between a *S. cerevisiae* cell and an *E. coli* cell. The volume of a particle can be calculated by:

$$\text{Volume}_{\text{sphere}} = \frac{4}{3}\pi R^3 \qquad 5.1$$

$$\text{Volume}_{\text{cylinder}} = \pi R^2 H \qquad 5.2$$

The volume of an *E. coli* calculated in Equation 5.2 is 5,300 times smaller than a larger 10μm yeast cell, and 670 times smaller than a 5μm yeast cell.

$$\text{Volume}(10\mu\text{m cell}) = \frac{4}{3}\pi R^3 = \frac{4}{3}\pi(10\mu\text{m})^3 \qquad 5.3$$

$$V(10\mu\text{m}) = 4189\mu\text{m}^3$$

$$\text{Volume}(0.5\text{x}1.\mu\text{m rod}) = \pi R^2 H = \pi(0.5\mu\text{m})^2(1\mu\text{m})$$

$$V(0.5\text{x}1\mu\text{m}) = 0.79\mu\text{m}^3$$

$$\text{Hence } \frac{V(10\mu\text{m})}{V(0.5\text{x}1\mu\text{m})} = \frac{4189\mu\text{m}^3}{0.79\mu\text{m}^3} = 5333$$

Simply, given the same acoustic driving pressure, then F_{ac} on yeast versus bacteria are between 670 and 5333 times smaller than the pressure on *S. cerevisiae* yeast according to:

$$F_{ac}\text{Yeast} = (\text{Volume}_{\text{Yeast}})(\text{Driving Pressure in Chamber}) \qquad 5.4$$

$$F_{ac}\text{Bacterium} = \left(\frac{1}{670} \text{ to } \frac{1}{5333}\right)(F_{ac}\text{Yeast})$$

Volume throughput was significant to the percent concentration because more yeast had the ability to be trapped in the chamber. It is believed that a higher volume of yeast suspension can be passed through for a greater percent concentration, but the equipment on hand did not provide for larger volumes to be tested in a reasonable manner.

Resonant Frequencies were, surprisingly, not found to be significant. It was believed that the higher the frequency, the shorter the wavelength – which provided for more nodal planes for the particles to move towards and also less distance to travel to get to those nodal planes.

Foam Density was also found not to be significant. Similar to the higher resonant frequencies, it was believed the higher the foam density, the more crevices there would be for the yeast to be trapped in with the ultrasonic forces. However, the confounding issue was with the reflecting power. It is believed the higher foam densities created greater impedance in the chamber which effectively decreased the sound pressure forces that would trap the yeast.

The Initial Concentration of yeast was not found to be significant and is explained by the methodologies used to calculate percent concentrated and percent clarified (which were proportional to the initial starting concentration). While the higher initial concentrations did in fact concentrate more yeast cells compared to the lower initial concentrations, correlating those concentrated values back to the starting concentrations and expressing the values as percentages eliminated the numerical values of yeast cells from influencing the results. Again, different initial starting concentrations of *E. coli* were not tested because of the way the numbers were calculated and furthermore because the one log-cycle between the maximum and minimum concentrations that could be detected via the Optical Density Detector was deemed as irrelevant to test.

After the "ideal" conditions were found to be 2000 VAC to the piezoceramic disc, driven at a frequency of 1560 kHz, using 200 mL of particle suspension with voltage applied, a flow rate of 8 mL min^{-1}, and a 45 PPI foam density, it was noticed the concentration efficiency increased as compared to the one-way factorials while only testing one variable at a time.

The drag forces and acoustic radiation forces act against each other. It is worth noting that the drag force on a particle in a slow flowing fluid field is a linear relationship to the radius and fluid velocity, while the effective volume (and acoustic radiation force) decreased as a cubic relationship. In the case of spherical particles with the same densities, the net force on particles result in a squared relationship with the radius. The change in radius from *S. cerevisiae* to *E. coli* is approximately a 10-fold decrease in radius, a 10-fold decrease in fluid drag force, and a 1000-fold decrease in acoustic radiation force; accounting for the decrease in drag and the decrease in acoustic radiation forces together, the net concentration force acting on the *E. coli* would be approximately 100-fold lower. However, to compound the issue, a rod-shaped *E. coli* can have different effective radius and drag force depending on its orientation against the fluid flow.

Future work would include use of a spherical bacterium, thus eliminating the confounding issue of various drag forces depending on cell orientation. The use of a third piezoceramic transducer perpendicular to the chamber might provide more information about the proper calibration of the frequency to the temperature to create a steady standing wave. Alternatively, a cooling methodology or an insulation layer between the piezoceramic and the fluid chamber could be implemented – however, the insulation layer would decrease the ability of the piezoceramic to transmit ultrasonic force into the chamber. Use of a larger chamber and additional flow-diffusion would be able to decrease the fluid velocity and thusly the drag forces while allowing for less contact with the heat generated from the piezoceramic.

CHAPTER 6 : CONCLUSIONS

The Ultrasonic Concentration prototype was tested for the effects of frequency, flow rate, initial concentration, volume throughput, voltage application, and polyurethane foam pore density on the concentration efficiency of microparticles. The prototype was found to be able to concentrate 10μm polystyrene beads and *S. cerevisiae* yeast cells; however, concentration of *E. coli* cells was transient and depended on temperature rise in the chamber.

Flow Rate, Voltage Input, and Volume Throughput were found to be the process variables that affected concentration of *S. cerevisiae*; a yeast suspension was clarified by as much as 69% and concentrated by as much as 200%

None of the process variables were found to be statistically significant for *E. coli*; an *E. coli* suspension was clarified by as much as 10% and concentrated by as much as 10%.

The poor concentration efficiency of *E. coli* as compared to the *S. cerevisiae* yeast cells is considered to be a result of the increased fluid drag forces and reduced acoustic radiation force per cell due to difference in cell volume.

APPENDICES

Appendix A Optical Density Detector Design

A.1Parts List

- 1.375” Delrin
- 0.5” Diameter X 0.125” thick Quartz Discs
- 0.25-20 X 1.375” Socket head cap screws
- FDA-Compliant nylon barbed tube fittings for 0.125” ID tube and 10-32 threads
- Dash No. 011 O-rings 0.4375” OD with 0.070” width

A.2 View 1

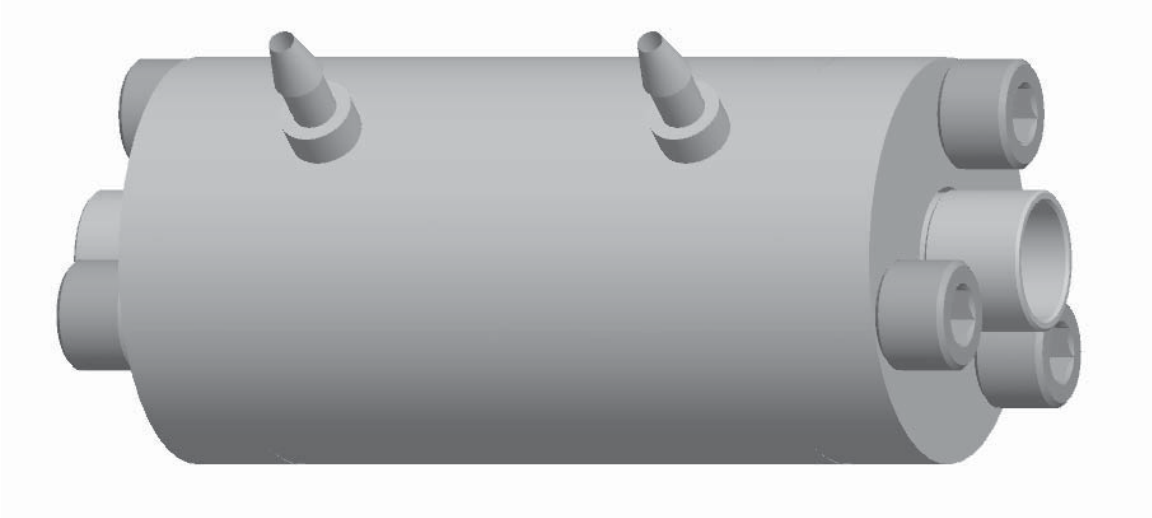

A.3 Wireframe View

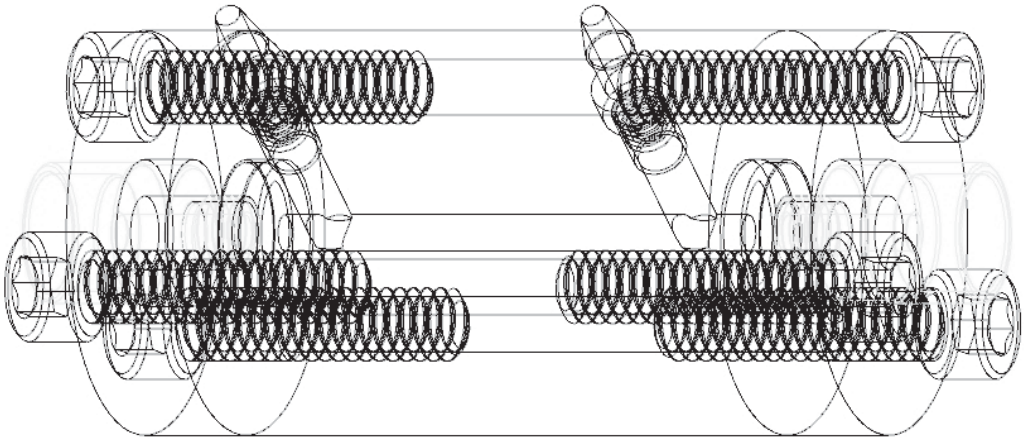

A.4 Cut-away view detailing the transmission and fluid path

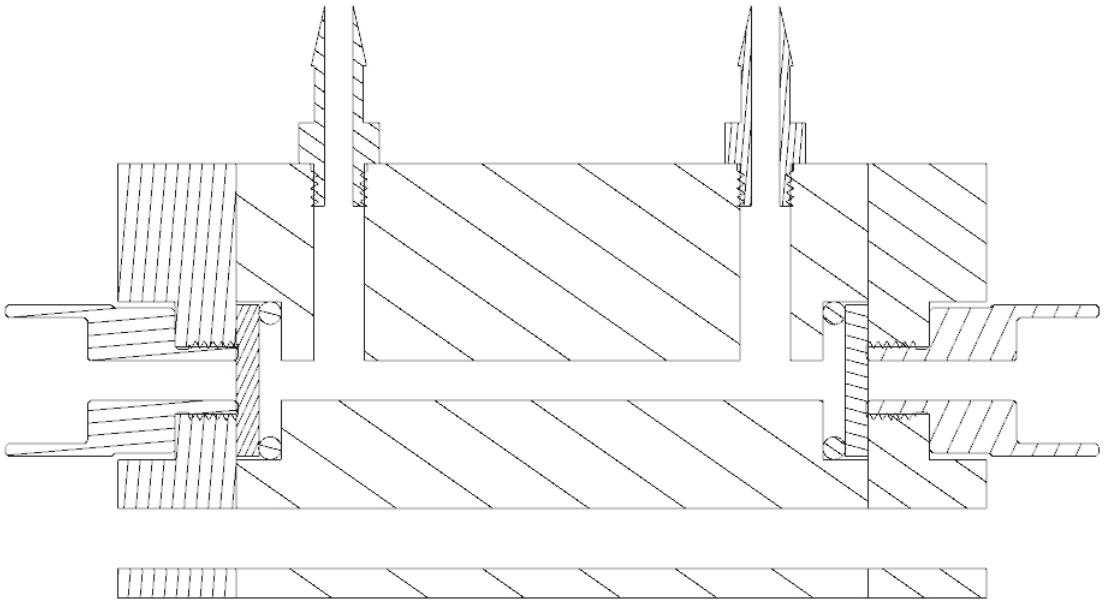

A.5 Exploded assembly drawing

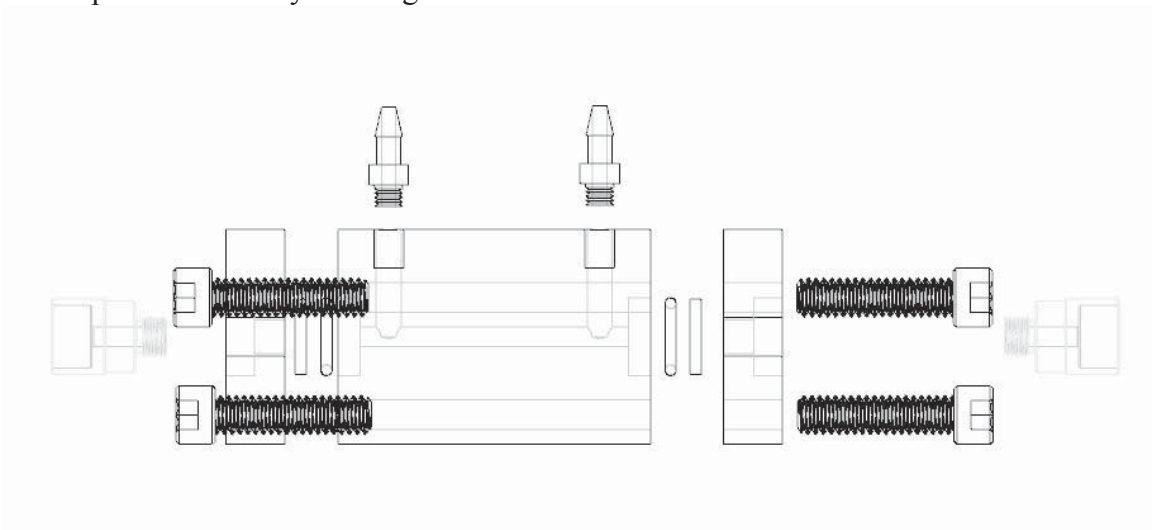

A.6 Dimensioned drawing of the 2” transmission tube

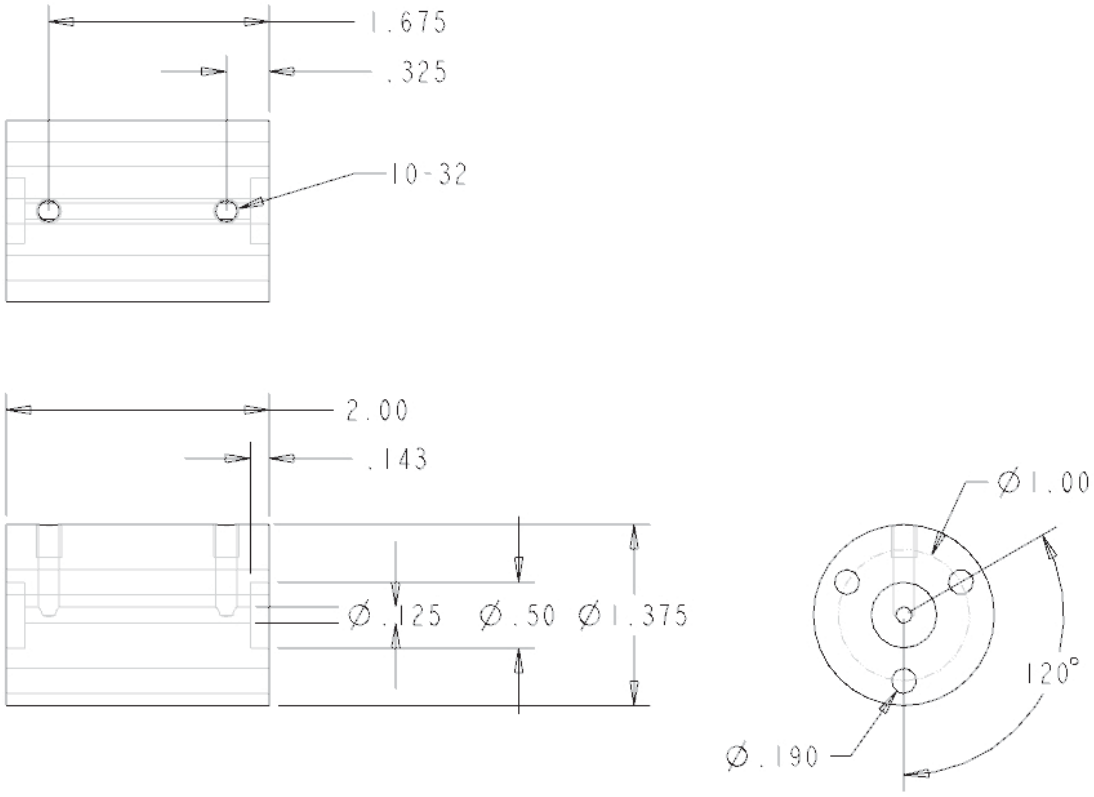

A.7 Dimensioned drawing of one of the two end-caps

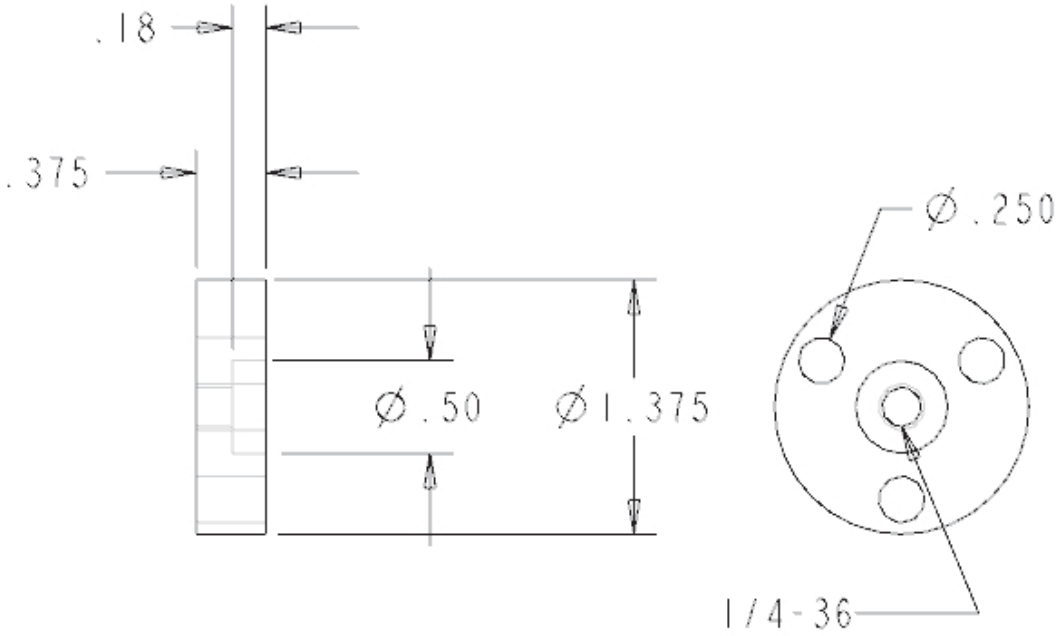

Appendix B Design of the Parallel Disc Ultrasonic Concentration prototype

B.1 CAD rendering of the prototype with in the custom stand

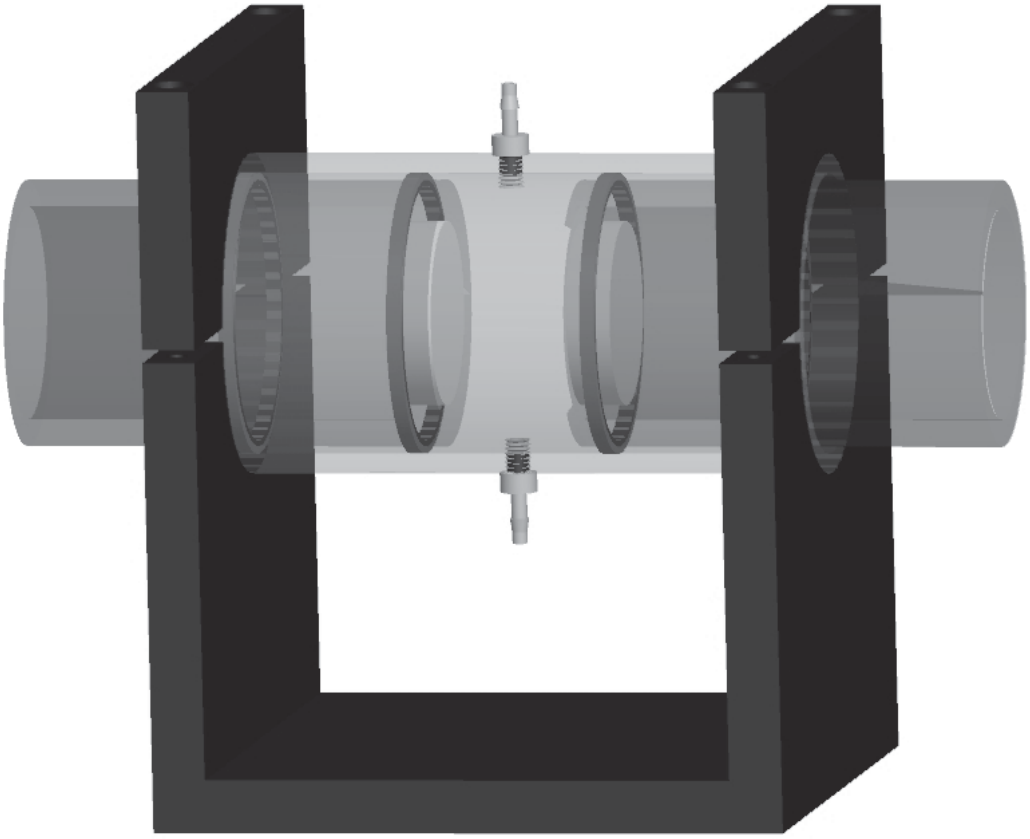

B.2 CAD rendering of the prototype showing the piezoceramic discs in yellow and O-rings in red

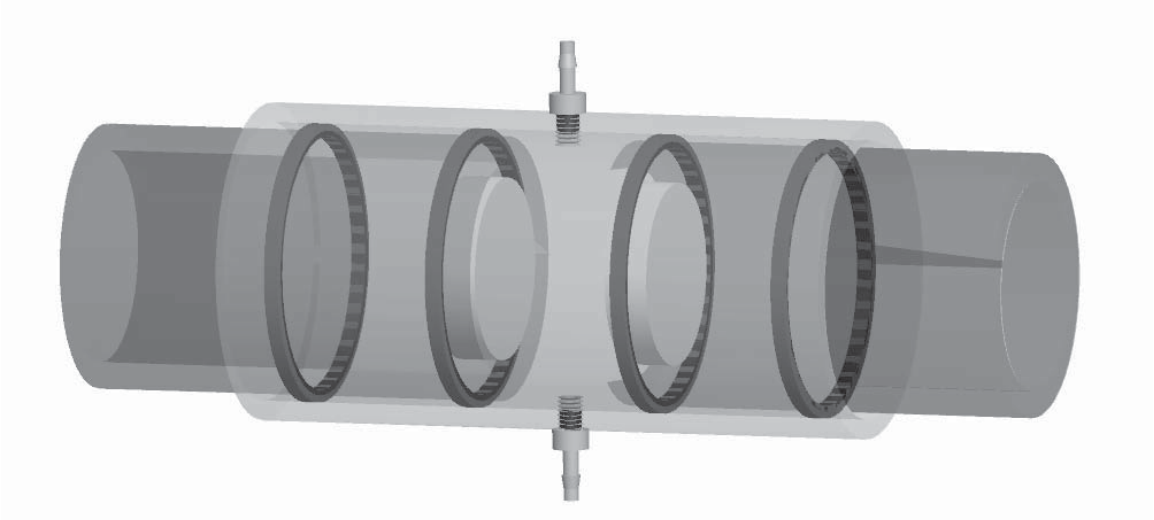

B.3 CAD rendering showing a front view

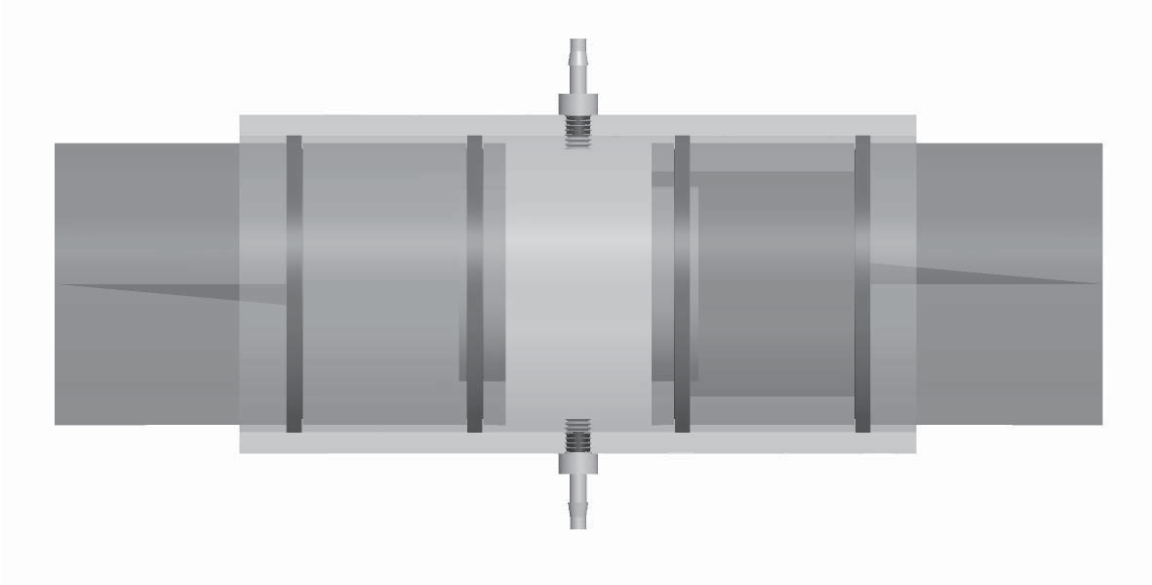

B.4 Cross-section view from the front.

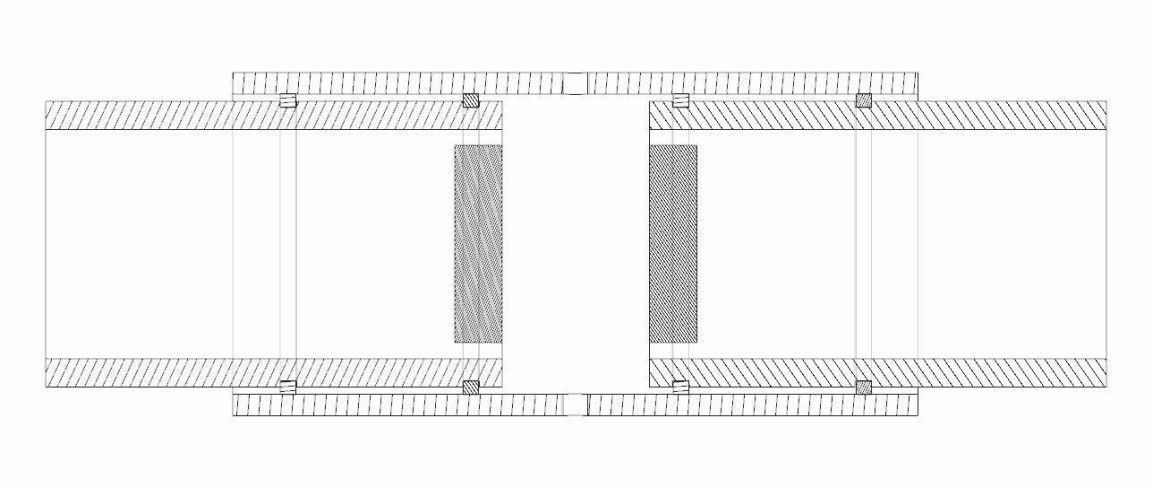

B.5 Dimensioned drawing for the outermost middle tube

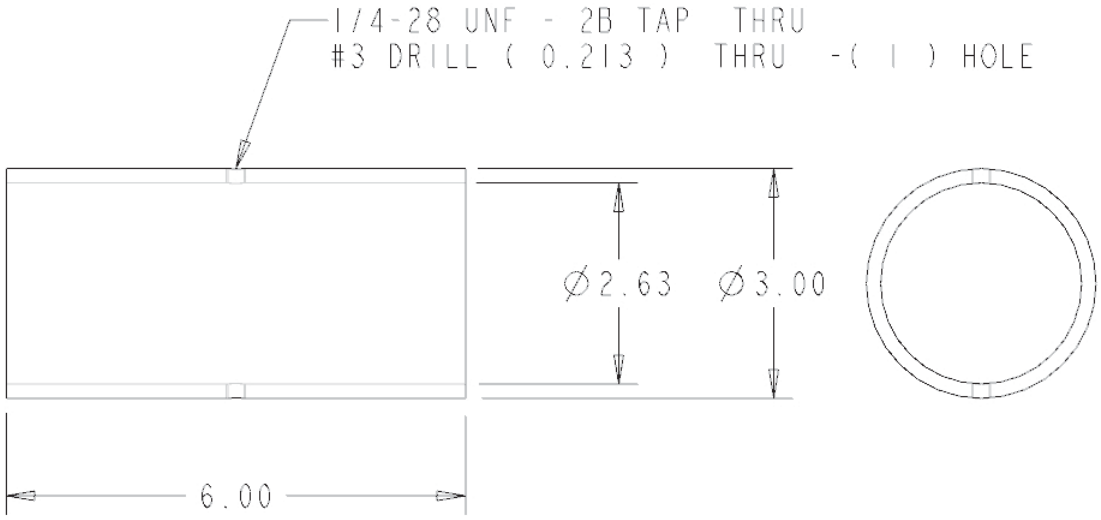

B.6 Dimensioned drawing for the two inner tubes holding a piezoceramic disc

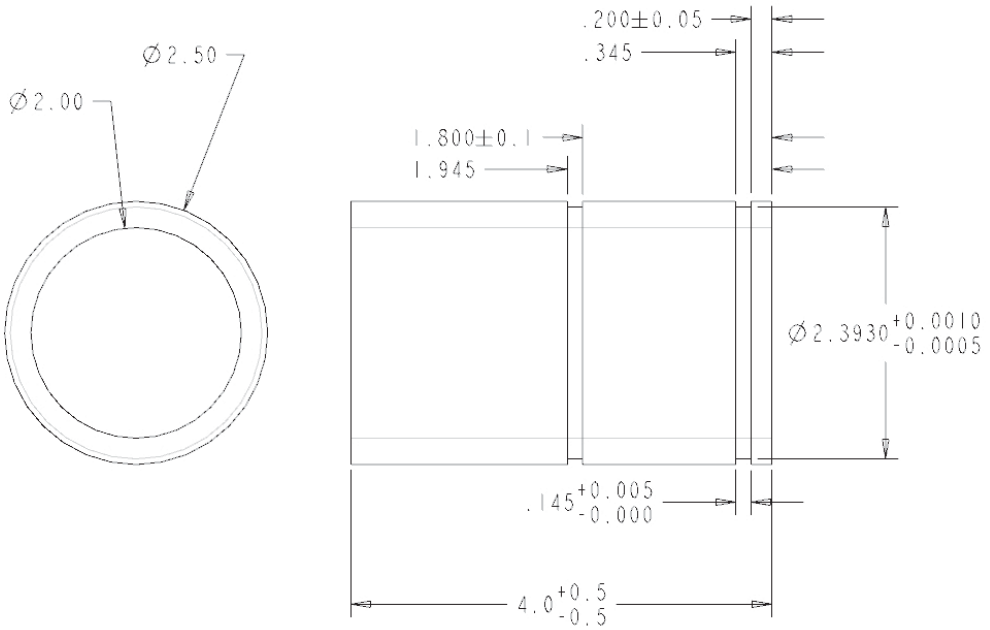

Appendix C Steiner and Martins PZT information

C.1 Information about the Piezo Ceramic Disc used in the Parallel Disc prototype

STEMiNC
STEINER & MARTINS, INC.

Piezo Ceramic Disc Voltage Generator

Part Number: SMD43T105F200S
Piezoelectric Ceramic disc. Silver electrodes being one on each side (S configuration). Thickness mode vibration application

Piezo Material: SM111
Dimensions: 43mm diameter x 10.5mm thickness
Resonant frequency f_r: 200 KHz±10 KHz

Electromechanical coupling coefficient K_p:≥40%
Resonant impedance Z_m: ≤10 Ω
Static capacitance C_s: 1700pF±15%@1kHz
Test Condition: 23±3 ºC 40~70% R.H.
f_r, Z_m, K_p => Thickness mode vibration application
C_s => LCR meter at 1KHz 1Vrms
Drawings: SMD43T105F200S,
Applications: Piezo transducer vibration, matter dispersion, Sonar Transducer Ultrasonic Sensor, Wall thickness sensor, Material stress sensor, Pressure sensor, Vibration generation, Piezo Energy Electricity harvesting, Piezo Electricity harvesting, Fish finder transducer, compression sensor, Piezo expansion sensor, biomedical probe and others.
Notes:
Old Part Number: SMD435T104F50NA

http://www.steminc.com/piezo/PZ_DiscViewPN.asp?PZ_Type=PIEZO%20DISC&PZ_SM_MODEL=SMD43T105F200S

C.2 Piezo Ceramic properties of the SM111 material used in the Piezo Ceramic Disc

PROPERTY	UNIT	SYMBOL	SM111
EQUIVALENCE			Modif. PZT-4
			N/A
OLD SYMBOLS			SMQA
Electromechanical coupling coefficient		K_p	0.58
		K_t	0.45
		K_{31}	0.34
Frequency constant	Hz • m	N_p	2200
		N_t	2070
		N_{31}	1680
Piezoelectric constant	$\times 10^{-12}$m/v	d_{33}	320
		d_{31}	-140
	$\times 10^{-3}$Vm/N	g_{33}	25
		g_{31}	-11.0
Elastic Constant	$\times 10^{10}$N/m^2	Y_{33}	7.3
		Y_{11}	8.6
Mechanical Quality Factor	-----	Q_m	1800
Dielectric Constant	@1KHz	$\varepsilon^T{}_{33/\varepsilon\ 0}$	1400
Dissipation Factor	%@1KHz	tan δ	0.4
Curie Temperature	°C	T_c	320
Density	g/cm^3	ρ	7.9

http://www.steminc.com/piezo/PZ_property.asp

C.3 Manufacturer Drawing of the Piezo Ceramic Disc

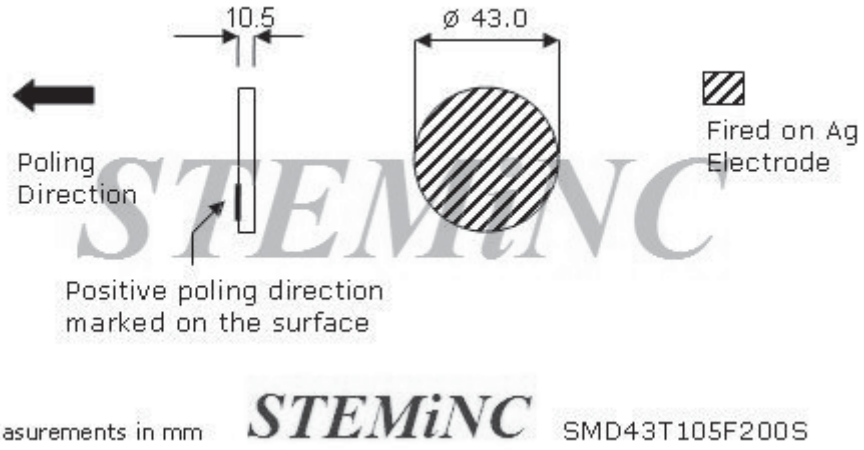

http://www.steminc.com/piezo/waterSpecs.asp?PZ_SM_MODEL=SMD43T105F200S

Appendix D Cylindrical Prototype

D.1 Three views of the Cylindrical Prototype to give and overview

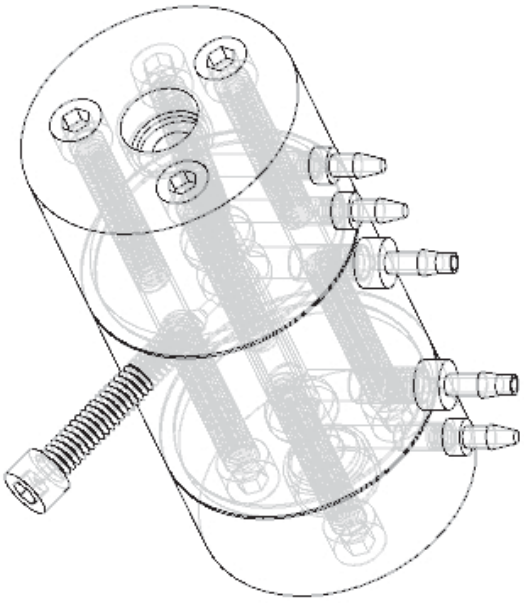

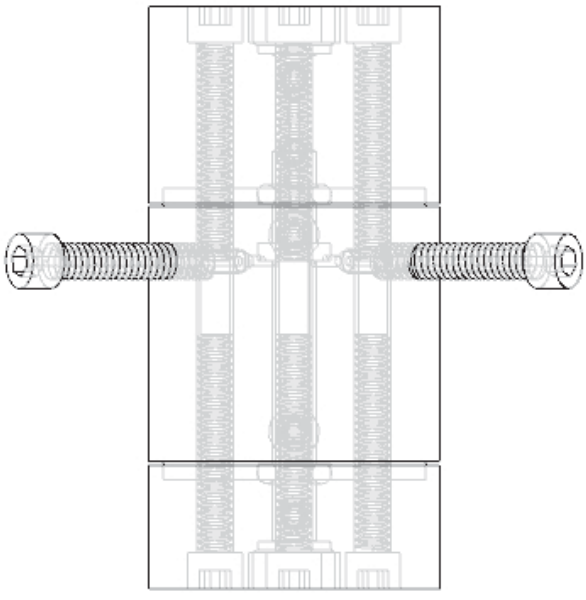

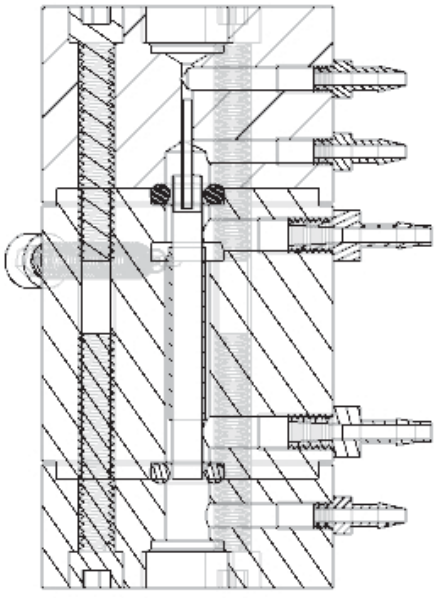

D.2 2D cross-section with colors for the cooling fluid and concentrated fluid

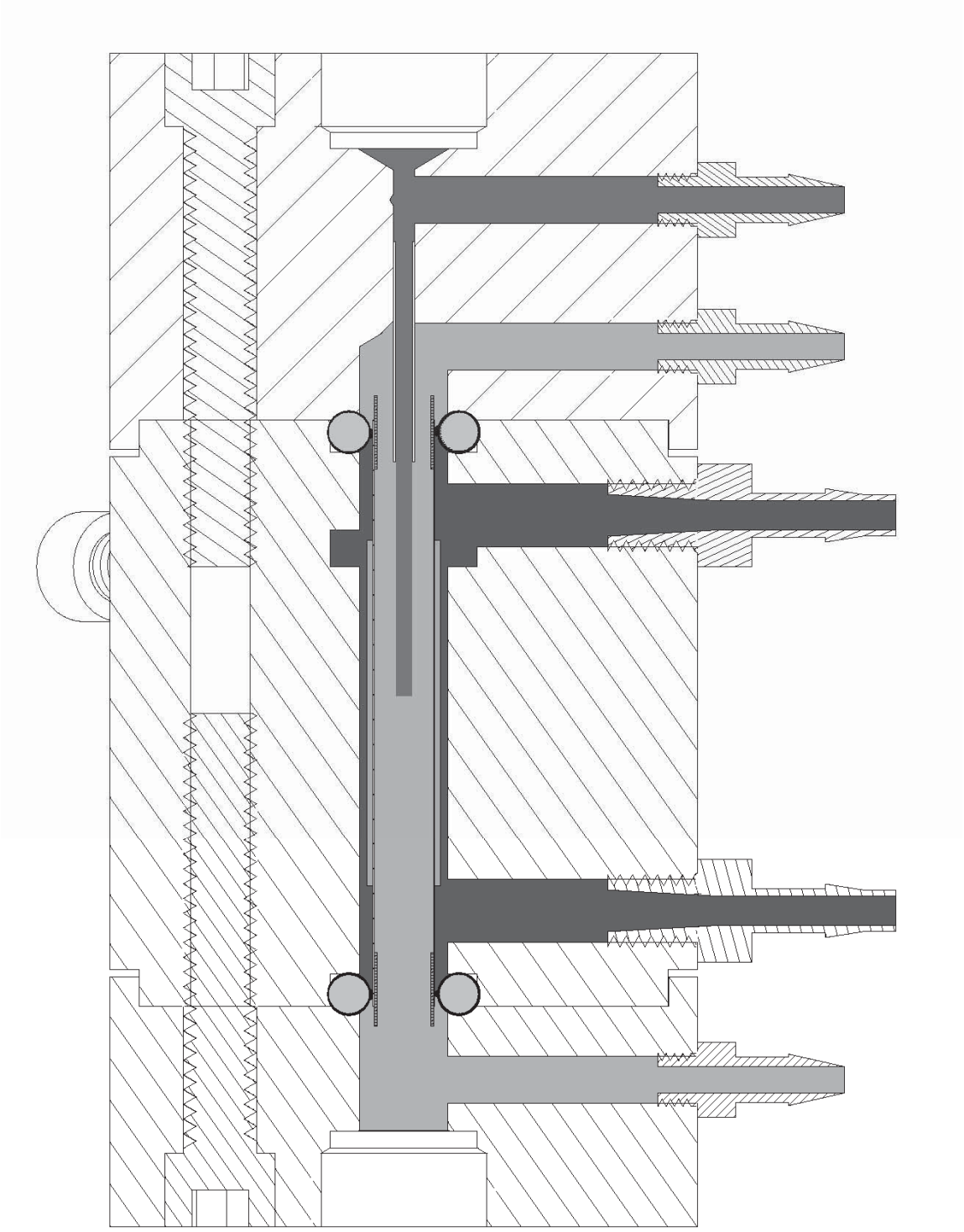

Blue: cooling fluid; light red: initial concentration of media; red: concentrated media; green: piezoceramic cylinder.

D.3Dimensioned drawing of the top section

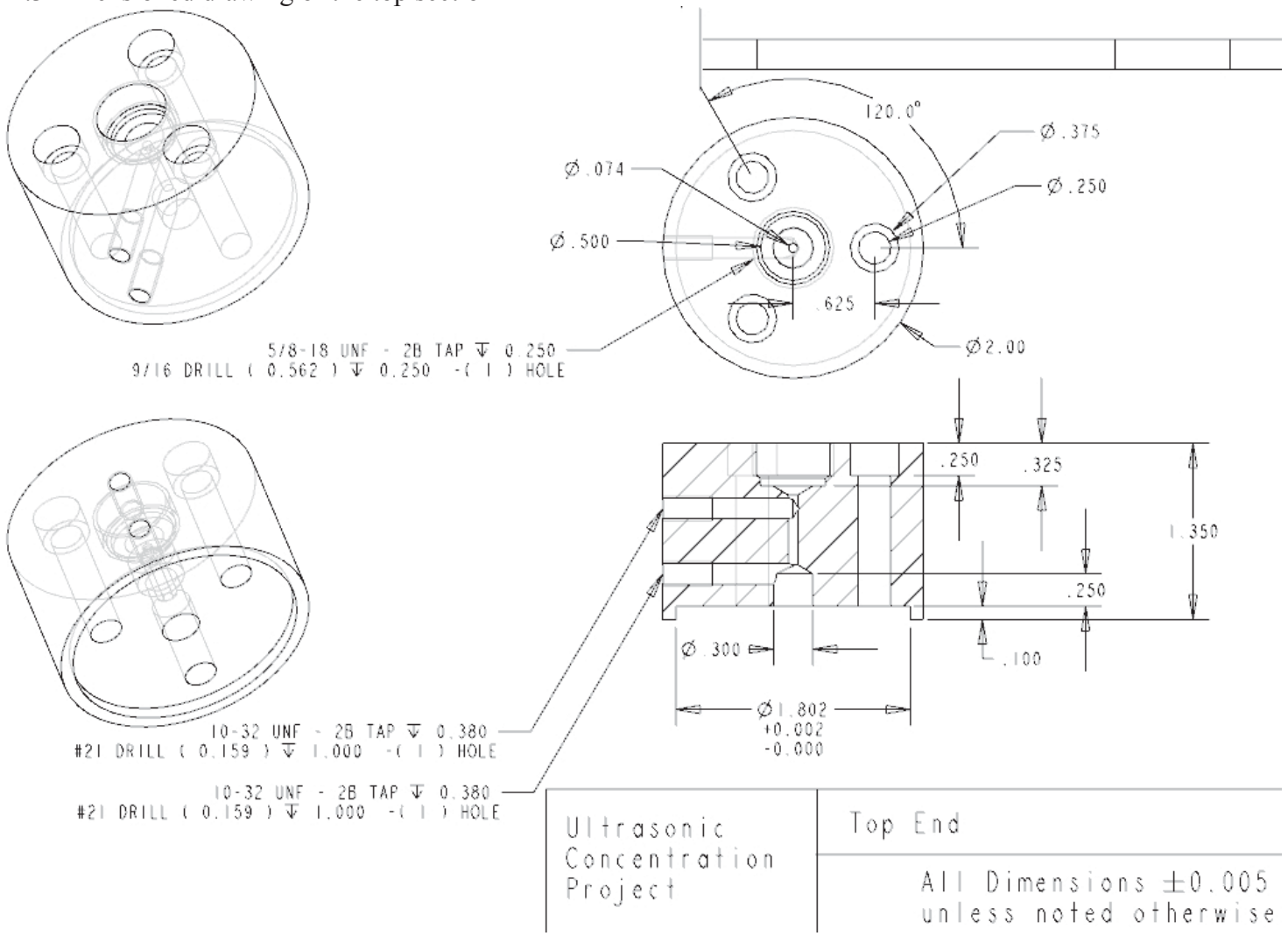

D.4Dimensioned drawing of the middle section

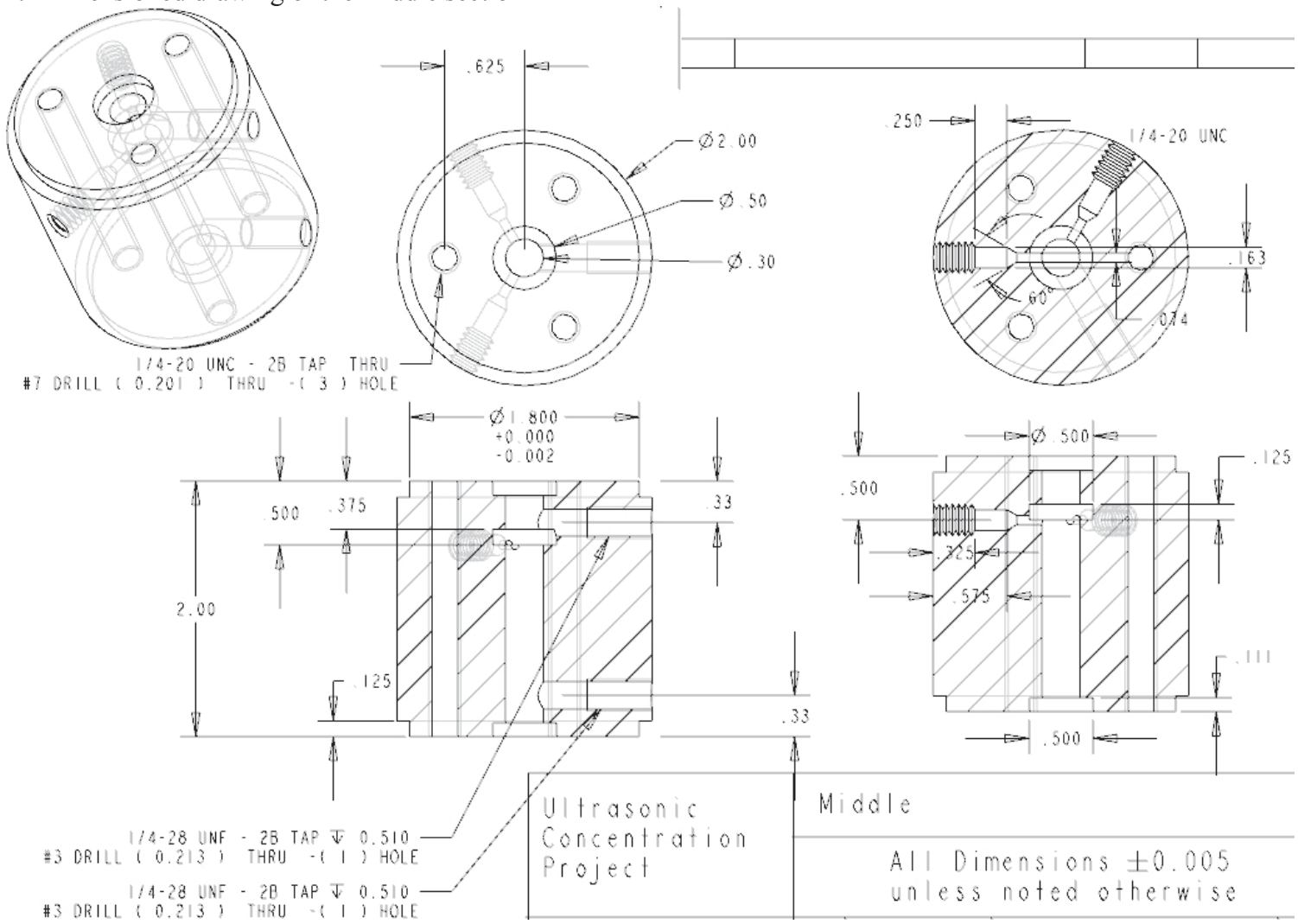

D.5 Dimensioned drawing of the bottom section

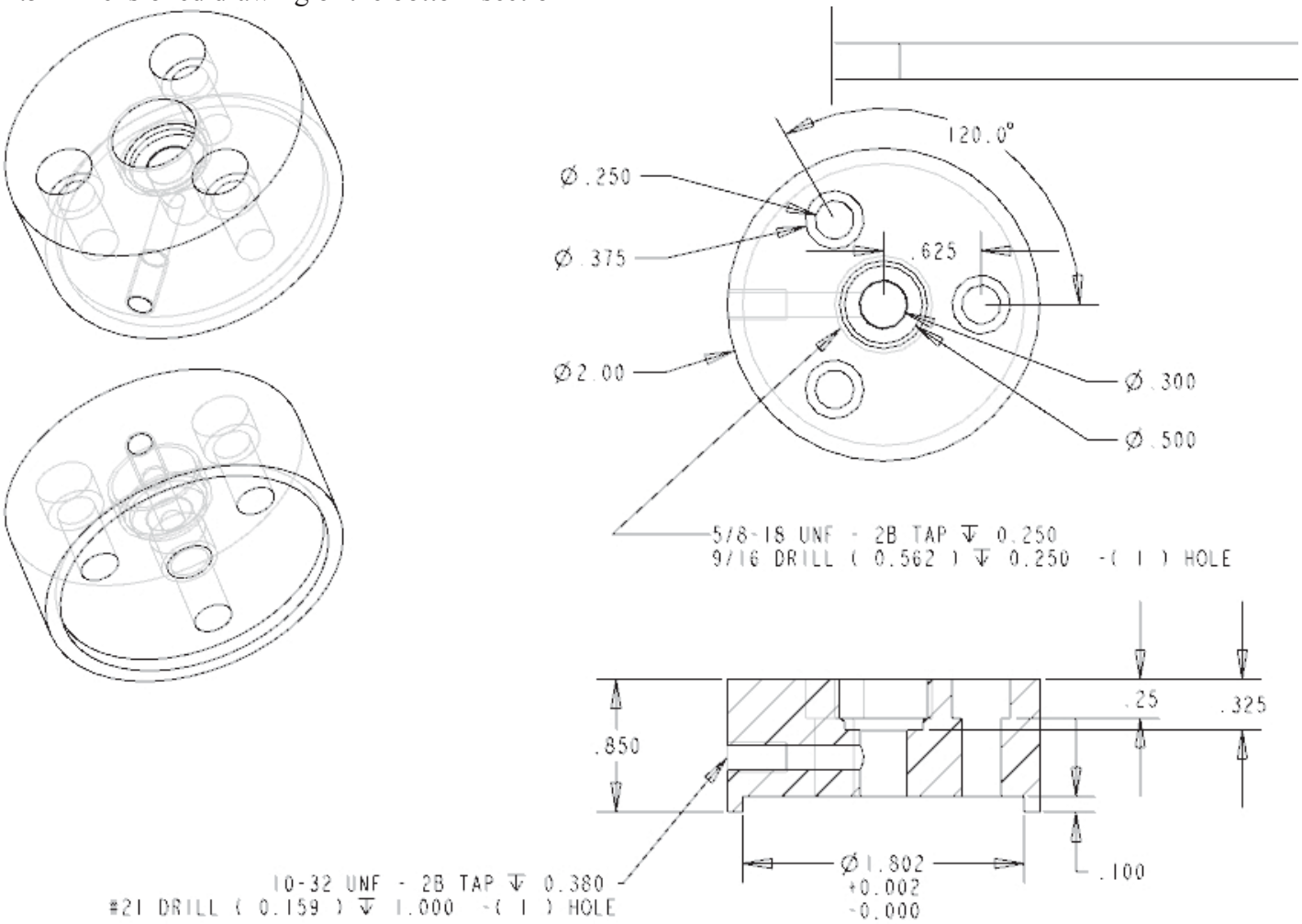

REFERENCES

Aboobaker, N., J. Meegoda, and, D. Blackmore. 2003. Fractionation and Segregation of Suspended Particles Using Acoustic and Flow Fields. *Journal of Environmental Engineeing.* 129(5), 427–434.

APC International Ltd. 2002. Piezoelectric Ceramics: Primciples and Applications. Mackeyville: APC Internationl, Ltd. 112 p.

Baldwin W. and H. Kubitschek. 1984. Buoyant Density variation during the cell cycle of Saccharomyces cerevisiae. *Journal of Bacteriology.* 158(2):701-704.

Bazou, D., L. Kuznetsova, W. Coakley. 2005. Physical environment of 2-D animal cell aggregates formed in a short pathlength ultrasound standing wave trap. *Ultrasound in Medicine andBiology.* 31:423-430.

Benes, E., M. Groschl, N. Nowotny, F. Trampler, T. Keijzer, H. Bohm, S. Rade, L. Gherardini, J. Hawkes, R. Konig, and C. Delouvroy. 2001. Ultrasonic Separation of Suspended Particles. *Proceedings of IEEE Ultrasonics Symposium.* 1:649-659.

Coakley, W. 1997. Ultrasonic separations in analytical biotechnology. *Trends in Biotechnology.* 15(12):506-511.

Cousins, C., J. Melin, W. Venables, and T. Coakley. 2001. Investigation of two processes, sedimentation and conjugation, when bacteria are concentrated in ultrasonic standing waves. *Bioseparation.* 9:343-349.

Danao, Mary-Grace Cachuela. 2005. Enhanced Optical Detection of Microparticles and Bacterial Cells in water using Stationary Acoustic wave fields. Dissertation, Doctorate of Philosophy, University of Kentucky.

Doblhoffdier, O., T. Gaida, H. Katinger, W. Burger, M. Groschl, and E. Benes. 1994. A novel ultrasonic resonancs field device for the retention of animal-cells. *Biotechnology Progress*. 10(4):428-432.

Doinikov, A. 1997. Acoustic radiation force on a spherical particle in a viscous heat-conducting fluid. *Journal of the Acoustical Society of America. 101:713-740.*

Embleton, T. 1954. Mean force on a sphere in a sphereical sound field, I (Theoretical). *Journal of the Acoustical Society of America.* 26:40-35.

Feke, D. and Z. Mandralis. 1993. Fractionation of Suspensions Using Synchronized Ultrasonic and Flow Fields. *AIChE Journal.* 39(2):197-206.

Gaida, T., O. Bonlhoftfdier, K. Strutzenberger, H. Katinger, W. Burger, M. Groschl, B. Handl, and E. Benes. 1996. Selective retention of viable sells in ultrasonic resonance field devices. *Biotechnology Progress.* 12:73-76.

Glynne-Jones, P., R. Boltryk, N. Harris, A. Cranny, and M. Hill. 2010. Mode-switching: A new technique for electronically varying the agglomeration position in an acoustic particle manipulator. *Ultrasonics.* 50:68-75.

Goddard, G. and G. Kaduchak. 2005. Ultrasonic particle concentration in a line-driven cylindrical tube. *Journal of the Acoustical Society of America.*117(6):3440–3447.

Gor'kov, L. 1962. On the forces action on a small particle in an acoustical field in an ideal fluid. *Soviet Physics.* 6:773-775.

Groschl, M. 1998a. Ultrasonic Separation of Suspended Particles – Part I: Fundamentals. *Acustica.* 84:432-447.

Groschl, M. 1998b. Ultrasonic Separation of Suspended Particles – Part II: Design and Operation of Separation Devices. *Acustica.* 84:632-642.

Groschl, M., W. Burger, B. Handel, O. Doblhoff-Dier, T. Gaida, and C. Schmatz. 1998. Ultrasonic Separation of Suspended Particles – Part III: Application in Biotechnology. *Acustica.* 84:815-822.

Grossner, M., A. Penrod, J. Belovich, and D. Feke. 2003. Single fiber model of particle retention in an acoustically driven porous mesh. *Ultrasonics.* 41:65-74.

Grossner, M., J. Belovich, and D. Feke. 2005. Transport analysis and model for the performance of an ultrasonically enhanced filtration process. *Chemical Engineering Science.* 60(12):3233–3238.

Gupta, S. and D. Feke. 1997. Acoustically driven collection of suspended particles within porous media. *Ultrasonics.* 35:131-139.

Gupta, S. and D. Feke. 1998. Filtration of particulate suspensions in acoustically driven porous media. *AIChE Journal.* 44(5):1005–1014.

Hawkes, J. and W. Coakley. 1996. A continuous flow ultrasonic cell-filtering method. *Enzyme and Microbial Technology.* 19(1):57-62.

Hawkes, J. and W. Coakley. 2001. Force field particle filter, combining ultrasound standing waves and laminar flow. *Sensors and Actuators.* 75:213-222.

Hawkes, J., M. Limaye, and W. Coakley. 1997. Filtration of bacteria and yeast by ultrasound-enhanced sedimentation. *Journal of Applied Microbiology.* 82:39-47.

Harris, N., M. Hill, S. Beeby, Y. Shen, N. White, J. Hawkes, and W. Coakley. 2003. A Silicon Microfluidic Ultrasonic Separator. *Sensors and Actuators.* 95:425-434.

Hill, M. and N. Harris. 2008. Ultrasonic microsystems for bacterial cell manipulation. In: Zourob M, Elwary S, Turner A, editors. Principles of bacterial detection: Biosensors, recognition receptors and microsystems. New York: Springer. P. 909-928.

Hill, R., A. Polaczyk, D. Hahn, J. Narayanan, T. Cromeans, J. Roberts, and J. Amburgey. (2005), Development of a rapid method for simultaneous recovery of diverse microbes in drinking water by ultrafiltration with sodium polyphosphate and surfactants. *Applied Environmental Microbiology.* 71:6878–6884.

Jaykus, L. 2003. Challenges to Developing Real-Time Methods to Detect Pathogens in Foods. *American Society for Microbiology News.* 69:341-347.

Kaduchak, G., D. Sinha, and D. Lizon. 2002. Novel cylindrical, air-couple acoustic levitation/concentration devices. *American Institure of Physics.* 73(3):1332-1336.

King, L. 1934. On the acoustic radiation pressure on spheres. *Proceedings of Royal Society of London.* 147:212–240.

Kundt, A. and O. Lehman. 1874. Longitudinal vibration and acoustic figures in cylindrical columns of liquids. *Annal Physik*. 153: 1-11.

Limaye, M., Hawkes, J., and Coakley, W. 1996. Ultrasonic standing wave removal of microorganisms from suspension in small batch systems. *Journal of Microbiological Methods.* 27:211-220.

Leung, E., N. Jacobi, and T. Wang. 1981. Acoustic radiation force on a rigid sphere in a reonance chamber. *Journal of the Acoustical Society of America.* 70(6): 1762-1767.

Martinez-Salas, E., J. Martin, and M. Vicente. 1981. Relationship of Escherichia coli density to growth rate and cell age. *Journal of Bacteriology.* July; 147(1); 97-100.

Nyborg, W. 1967. Radiation pressure on a small rigid sphere. *Journal of the Acoustical Society of America.* 42:947-952.

Petersson, F., A. Nilsson, C. Holm, H. Jonsson, and T. Laurell. 2004. Continuous separation of lipid particles from erythrocytes by means of laminar flow and acoustic standing wave forces. Lab on a Chip. 5(1):20-22.

Peterson, F., A. Nilsson, H. Jonsson, and T. Laurell. 2005. Carrier medium exchange through ultrasonic particle switching in microfluidic channels. *Analytical Chemistry.* 77:1216-1221.

Serway, R. and J. Jewett. 2004. Physics for Scientists and Engineers. 6th ed. Belmont: Brooks/Cole-Thomson Learning. 1283 p.

Toubal, M., M. Asmani, E. Radziszewski, and B. Nongaillard. 1999. Acoustic measurement of compressibility and thermal expansion coefficient of erythrocytes. *Physics in Medicine and Biology.* 44(5):1277-1287.

Wang, Z., P. Grabenstetter, D. Feke, and J. Belovich. 2004. Retention and viability characteristics of mammalian cells in an acoustically driven polymer mesh. *Biotechnology Progress.* 20(1):384–387.

Westervelt, P. 1957. Acoustic radiation pressure. *Journal of the Acoustical Society of America.* 29(1):26–29.

Whitworth, G., M. Grundy, and W. Coakley. 1991. Transport and harvesting of suspended particles using modulated ultrasound. *Ultrasonics.* 29(6):439–444.

Yasuda, K. and T. Kamakura. 1997. Acoustic radiation force on micrometer-size particles. *American Institute of Physics.* 71(13):1771-1773.

Yosioka, K, and Y. Kawasima. 1955. Acoustic radiation pressure on a compressible sphere. *Acustica.* 5:167–173.

Zhou, C., P. Pivarnik, A. Rand, and S. Letcher. 1998. Acoustic standing-wave enhancement of a fiber-optic *Salmonella* biosensor. *Biosensors & Bioelectronics.* 13:495-500.

VITA

Samuel James Mullins

PERSONAL
Born February 27th, 1987

EDUCATION
B.S. in Biosystems and Agricultural Engineering, University of Kentucky, Lexington, KY, May 2009.

EXPERIENCE
Associate Engineer, Biosystems and Agricultural Engineering Department, University of Kentucky. July 2009 to August 2012. Supervisor: Dr. F. A. Payne.

Undergraduate Research Assistant, Biosystems and Agricultural Engineering Department, University of Kentucky. January 2009 to July 2009. Supervisor: Dr. F. A. Payne.

Undergraduate Research Assistant, Departamento de Engenharia Agricola, Universidade de Viçosa, Brazil. Supervisor: Dr. E. Alvez.

Undergraduate Extension Research Assistant, Biosystems and Agricultural Engineering Department, University of Kentucky, Princeton, KY. May 2008 to August 2008. Supervisor Dr. D. G. Overhaults.

Undergraduate Laboratory Research Assistant, DeBakey Institute, Texas A&M, College Station Texas. Supervisor: Dr. C. M. Quick.

Undergraduate Laboratory Research Assistant, Biosystems and Agricultural Engineering Department, University of Kentucky. May 2006 to August 2006. Supervisor: Dr. C. L. Crofcheck.

Cable Harness Assembler, Machine Drive Company, Blue Ash Ohio. May 2005 to August 2005. Supervisor: B. Ashley.

HONORS
Engineer in Training Certificate. May 2008.

TECHNICAL PRESENTATIONS
Mullins, S., F. Payne, and M. Danao. 2012. Ultrasonic Concentration of Microbial Pathogens using Piezoceramic Discs and Semi-Continuous Flow. ASABE Annual International Meeting in Dallas, TX, August 2012.